

12-1-2018

# Effect of Humidity and testing strategy on Friction Performance of model brake pads containing Nano-additives

SaiKrishna Kancharla

*Southern Illinois University Carbondale*, saikrishna.kancharla@siu.edu

Follow this and additional works at: <https://opensiuc.lib.siu.edu/theses>

## **Related Files**

[thesis files.zip](#) (7855 kB)

---

## **Recommended Citation**

Kancharla, SaiKrishna, "Effect of Humidity and testing strategy on Friction Performance of model brake pads containing Nano-additives" (2018). *Theses*. 2456.

<https://opensiuc.lib.siu.edu/theses/2456>

This Open Access Thesis is brought to you for free and open access by the Theses and Dissertations at OpenSIUC. It has been accepted for inclusion in Theses by an authorized administrator of OpenSIUC. For more information, please contact [opensiuc@lib.siu.edu](mailto:opensiuc@lib.siu.edu).

EFFECT OF HUMIDITY AND TESTING STRATEGY ON FRICTION PERFORMANCE OF  
MODEL BRAKE PADS CONTAINING NANO-ADDITIVES

by  
Sai Krishna Kancharla

B.Tech, Jawaharlal Nehru Technological University, 2016.

A Thesis  
Submitted in Partial Fulfillment of the Requirements for the  
Master of Science Degree

Department of Mechanical Engineering and Energy Processes  
in the Graduate School  
Southern Illinois University Carbondale  
December 2018

THESIS APPROVAL

EFFECT OF HUMIDITY AND TESTING STRATEGY ON FRICTION PERFORMANCE OF  
MODEL BRAKE PADS CONTAINING NANO-ADDITIVES

by

Sai Krishna Kancharla

A Thesis Submitted in Partial  
Fulfillment of the Requirements  
for the degree of  
Master of Science  
in the field of Mechanical Engineering and Energy Processes

Approved by:

Dr. Peter Filip, Chair

Dr. Rasit Koc

Dr. Steven Shaffer

Graduate School  
Southern Illinois University Carbondale  
October 31, 2018

## AN ABSTRACT OF THE THESIS OF

SAI KRISHNA KANCHARLA, for the Master of Science degree in MECHANICAL ENGINEERING, Presented on October 31, 2018, at Southern Illinois University Carbondale

TITLE: EFFECT OF HUMIDITY AND TESTING STRATEGY ON FRICTION PERFORMANCE OF MODEL BRAKE PADS CONTAINING NANO-ADDITIVES

MAJOR PROFESSOR: Dr. Peter Filip

Interaction of friction brakes with external environment can considerably influence their performance which could relate to friction instabilities and friction induced vibration and noise. Humidity can alter the chemistry of friction surfaces that could relate to unwanted phenomena which may increase the cost of product. In addition to the chemical phenomena leading to unwanted reactions, there are physical effects related to adsorption of humidity and to modification of adhesion, accompanied with changes in contact surfaces and contact mechanics. The goal of this thesis is to address these chemical and physical phenomena occurring at friction interfaces of model friction materials modified by nano-additives and to relate them to their performance. Friction tests were performed by using the bench-top UMT TriboLab friction tester equipped with humidity and temperature chambers and scaled-down parameters derived from adopted real vehicle braking scenario. Wear surfaces/mechanisms were studied by using scanning electron microscopy equipped with the energy dispersive X-ray microanalysis, and 3D optical microscope. Vibrational response was monitored by triaxial ICP Accelerometer and Oscilloscope. The data were analyzed by use of Matlab. The physical adsorption is dependent strongly on the surface topography; nevertheless, the chemical species/products of complex reactions generated at the friction surfaces are the dominant factor dictating performance and the quantity of absorbed humidity/species. Chemistry of chemicals generated on friction surfaces

differs from the chemistry of bulk and a complex correlation between pad formulations and brake performance shall be further studied. Adsorption of humidity considerably influences the friction performance (friction and its stability, wear, noise and environmental response/pollution capacity) of brake pads. Presence of nano-additives made an impact on friction performance at elevated humidity conditions.

Keywords – nanomaterial additives, humidity, friction, scanning electron microscopy, brake pads and X-ray microanalysis.

## DEDICATION

I dedicate my thesis firstly to my family, my advisors and my friends who were with me all throughout the time. A feeling of gratitude to my loving parents, who have always loved me unconditionally and whose good examples have taught me to work hard for the things that I aspire to achieve. My sister, Sai Manohari Kancharla who always supported me and cared about me.

I also like to dedicate this thesis to Dr. Peter Filip who has been encouraging me into many new endeavors all throughout the time in this university. I will always remember the words of wisdom he has shared with me.

## ACKNOWLEDGEMENTS

I use this very opportunity to thank my academic advisor, Dr. Peter Filip who has not left any stone unturned for helping me out. This research would not have been possible without you Professor. Thank you!

I would also like to thank my committee members, Dr. Rasit Koc and Dr. Steven Shaffer for their immense support and guidance. I would also take this opportunity to thank them for reviewing my report.

I would like to thank Mr. Rohit Jogineedi for helping me gain all the necessary knowledge I need with the latest programming languages.

Finally, I would like to thank my friends and colleagues who have always supported and motivated me throughout my research work. It would not be possible to have continued with research without their love and encouragement.

TABLE OF CONTENTS

<u>CHAPTER</u>	<u>PAGE</u>
ABSTRACT .....	i
DEDICATION.....	iii
ACKNOWLEDGMENTS .....	iv
LIST OF FIGURES .....	vii
LIST OF TABLES.....	viii
CHAPTERS	
CHAPTER 1 – INTRODUCTION.....	1
CHAPTER 2 – LITERATURE REVIEW .....	7
CHAPTER 3 – STATEMENT OF OBJECTIVE .....	21
CHAPTER 4 – EXPERIMENTAL .....	22
CHAPTER 5- RESULTS AND DISCUSSION.....	28
CHAPTER 6- CONCLUSION .....	51
REFERENCES .....	52
VITA .....	58



## LIST OF FIGURES

<u>FIGURE</u>	<u>PAGE</u>
FIGURE 1 SCHEMATIC PICTURE OF DISC BRAKE. ....	2
FIGURE 2 ILLUSTRATION OF FRICTION FORCE.....	8
FIGURE 3 CONTACT SITUATION BETWEEN TWO ROUGH SURFACES.....	8
FIGURE 4 SCHEMATIC ILLUSTRATION OF A NORMAL FORCE $w$ , WHICH FORMS AN ADHESIVE FORCE AND A TENSILE FORCE $w'$ WHICH PULLS TO SEPARATE THEM [39].....	10
FIGURE 5 FORMATION OF MENISCI DUE TO CONDENSATION OF LIQUID MOLECULES [39] .....	11
FIGURE 6 REGIMES OF DIFFERENT LIQUID LEVELS [39] .....	12
FIGURE 7 POSSIBILITIES FOR SCALING TRIBO TESTING .....	15
FIGURE 8 LENGTH COMPARISON OF REAL BRAKE PAD TO PAD SAMPLE.....	18
FIGURE 9 (A) BUEHLER ISOMET 4000 AND (B) SAMPLE USED IN HOLDER.....	22
FIGURE 10 PEARLITIC CAST IRON ROTOR.....	23
FIGURE 11 SAMPLE HOLDER USED IN UMT.....	23
FIGURE 12 (A)UMT BENCH TOP TESTER (B) ACCELEROMETER AND MICROPHONE MOUNTING. ....	24
FIGURE 13 RUN IN PROCESS.....	26
FIGURE 14 FRICTION FORCE DURING RUN IN PROCESS.....	26
FIGURE 15 REAL BRAKING TEST FOR MODEL MATERIAL 1 (LM) .....	28
FIGURE 16 REAL BRAKING TEST FOR MODEL MATERIAL 2 (NAO) .....	29
FIGURE 17 DRAG TEST FOR MODEL MATERIAL 1 (LM).....	29
FIGURE 18 DRAG TEST FOR MODEL MATERIAL 2 (NAO).....	30

FIGURE 19 (A) SEM OF MODAL MATERIAL 1 AT 250X MAGNIFICATION, (B) BACK SCATTERED ELECTRON IMAGE FOR MODAL MATERIAL 1 AND (C) EDX ANALYSIS OF MODAL MATERIAL 1 AFTER FRICTION TESTS .....	32
FIGURE 20 (A) SEM OF MODAL MATERIAL 2 AT 250X MAGNIFICATION, (B) BACK SCATTERED ELECTRON IMAGE FOR MODAL MATERIAL 2 AND (C) EDX ANALYSIS OF MODAL MATERIAL 2 AFTER FRICTION TESTS .....	33
FIGURE 21 FFT ANALYSIS OF ACCELEROMETER (A), MICROPHONE (B) AND COF IN UMT (C) FOR MODAL MATERIAL 1 AT 15% RH .....	36
FIGURE 22 FFT ANALYSIS OF ACCELEROMETER (A), MICROPHONE (B) AND COF IN UMT (C) FOR MODAL MATERIAL 1 AT 65% RH .....	37
FIGURE 23 FFT ANALYSIS OF ACCELEROMETER (A), MICROPHONE (B) AND COF IN UMT (C) FOR MODAL MATERIAL 2 AT 15% RH .....	39
FIGURE 24 FFT ANALYSIS OF ACCELEROMETER (A), MICROPHONE (B) AND COF IN UMT (C) FOR MODAL MATERIAL 2 AT 65% RH .....	41
FIGURE 25 FFT ANALYSIS OF ACCELEROMETER (A), MICROPHONE (B) AND COF IN UMT (C) FOR MODAL MATERIAL 1 AT 15% RH .....	43
FIGURE 26 FFT ANALYSIS OF ACCELEROMETER (A), MICROPHONE (B) AND COF IN UMT (C) FOR MODAL MATERIAL 1 AT 65% RH .....	45
FIGURE 27 FFT ANALYSIS OF ACCELEROMETER (A), MICROPHONE (B) AND COF IN UMT (C) FOR MODAL MATERIAL 2 AT 15% RH .....	47
FIGURE 28 FFT ANALYSIS OF ACCELEROMETER (A), MICROPHONE (B) AND COF IN UMT (C) FOR MODAL MATERIAL 2 AT 65% RH .....	49

LIST OF TABLES

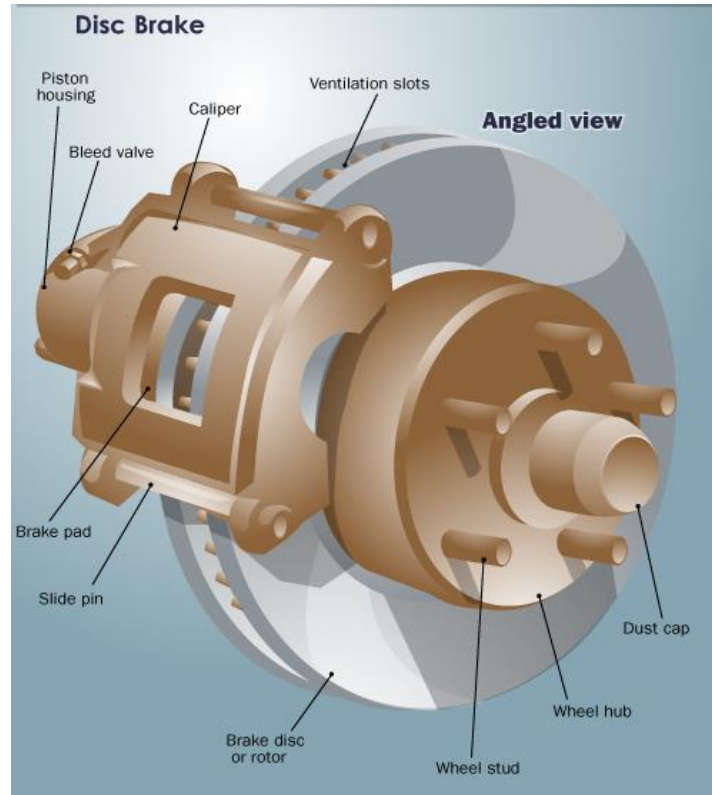
<u>TABLE</u>	<u>PAGE</u>
TABLE 1– SCALING IN DIFFERENT PARAMETERS.....	19

## CHAPTER 1

### INTRODUCTION

Friction is a force resisting relative movement of two materials in contact. Friction is determined by the system, by properties of the friction materials, by the character of the active surfaces of the disc and pad friction called friction layer. In automotive industry, friction is mainly observed in the braking applications. A friction brake is a mechanical device that reduces motion by absorbing kinetic energy and dissipating heat from a moving system [1]. It is used for slowing or stopping a vehicle in motion, most often accomplished by means of friction. Friction brakes normally utilize contact between two surfaces compressed together to change the kinetic energy of the moving item into heat, however different strategies for energy transformation might be utilized [2]. The two main type of brakes used in passenger vehicles are

- Disc brake system, consisting in pushing two brake pads on to a disc.
- Drum brake system, consisting in pushing outwards brake shoes mounted inside a drum against the inner surface of the drum.



*Figure 1 Schematic picture of Disc brake*

In present automotive vehicles, disc brakes are mostly used as they dissipate the heat more efficiently [3], so the current study is on the disc brakes. Modern light and commercial vehicles disc-pad brake systems are constituted by a brake disc, integral with the wheel hub, which is clamped by brake pads pushed on the disc by slave cylinders inside a caliper fixed to a hub bracket [3] see (Figure.1). Here, the kinetic energy of the vehicle is converted mostly to thermal energy [4].

Brake pad performance shall be defined by the following factors, which include friction level and stability, wear rate, propensity to generate vibrations and noise, and impact of wear debris on environment and health issues. One of the important factors that defines the effectiveness of braking is the brake pad material composition. Brake lining materials generally are asbestos, metals, non - asbestos organic (NAO) such as palm kernel shell (PKS), and

ceramics. Asbestos during application releases the hazardous gases, which causes health issues [5], this led to the ban of asbestos usage in brakes. In general, the brake pads are broadly classified into Non-asbestos organic, semi-metallic and low metallic types depending upon the material used in brake pads [6]. Typically, non-asbestos brake pads are made from organic materials such as glass, rubber and Kevlar, semi metallic brakes contain 30-65% of metals, finally, low steel contains less than 30% of steel [7]. Brake pad material composites can easily make use of the nanomaterials because of the small size of the particle. With the large surface area of nanomaterials very small quantities are needed to observe significant friction altering effects as observed by numerous researchers. Specifically, when the nanomaterials become part of the friction layer they will increase the contact area, the mechanical properties, reduces wear and typically increase and stabilizes the coefficient of friction [8]. Pearlitic cast iron is mostly used in brake rotors, one of the most important features of cast-iron brake discs from the disc operation point of view is the condition of the working (friction) surface of the disc as this surface is not homogenous, it is divided into areas of pearlitic and ferritic structure and other areas where graphite precipitates predominate. Due to this overall structure of the friction surface, vibrations with high frequencies are being damped [9].

Due to the increase in customers' needs for shorter stopping distance, ease of operation and high braking comfort (with low noise and vibration) is leading engineers continue developing friction materials matching the increasingly demanding safety, environmental and customer requirements [1]. Researchers strive hard to achieve a better braking experience along with a stable coefficient of friction when exposed to different braking conditions. Friction coefficient is a system property and is not completely depending on materials, rubbing against each other [10]. The entire system in which brake operates and other external conditions impact

their performance. Experimental studies demonstrated the impact of friction and wear performance of a given friction material. Dependency of friction coefficient on normal load, relative humidity, temperature, sliding friction, roughness of surfaces and nature of material, influence the real area of contact which impacts the friction coefficient [11]. Therefore, friction and wear are not simply materials parameters available in handbooks: they are unique characteristics of the tribological system in which they are measured [10]. Therefore, when performing tests relevant for development, care must be exercised.

In recent years, various authors have done research on the contact film for the disc brakes. The analytical representation of the pad- disc tribological contact is challenging, which in turn influences the brake operation by varying the coefficient of friction of the brake, fading [7] [12], bedding [13], hysteresis against the pressure, hysteresis against speed [2], wear [14, 15, 16] aging [13] and variation in the environmental condition [17], the behavior disc-pad coupling is also dependent on the chemical composition and mechanical properties of each brake component [18].

Once a brake pad is manufactured testing is very important in determining the effectiveness of the brake [19]. The testing consists of various on-field tests to laboratory tests such as dyno and other small-scale tests. But, the final test involves on vehicle tests equipped with full size components. Brake performance is affected not only by the materials and vehicle hardware design, but also significantly by driver behavior, the vehicle usage, the state of adjustment of the brake hardware, and the overall environment in which the vehicle is driven and no laboratory test can simulate driving conditions precisely [1]. The main purpose of testing is to simulate the laboratory tests as close as possible to the on-vehicle conditions on which the brake pad works. Majority of the standardized friction and wear testing procedures apply somehow

“empirical philosophy” to their testing scenarios [19, 7]. This included, for example, the standardized tests of friction and wear e. g. ASTM G99. Similarly, the recommended particles defining testing procedures, developed for assessment of brake performance of passenger cars e. g. SAE J2522, provide conditions to be used in automotive (“full-scale”) brake dynamometers, offering somehow generally adopted test philosophies based on agreement of professional committees and applied to a wide range of passenger vehicles [20].

In contrast to these strategies, adoption of the “proper scaling-down philosophy” based of laws of physics demonstrated that the results obtained on a small scale bench-top tester could correlate well with the findings generated using the full-scale automotive brake dynamometer performance tests data and their trends [7] [21, 22]. Although the scaling and related testing simulations do not aspire to offer a perfect prediction of friction performance in real systems, is certainly possible to make educated decisions particularly when “on the research and development stages” [23], which in turn could lead to considerable savings of time and financial resources. In addition to the usually controlled physical parameter like normal load (pressure), torque, sliding speed, and temperature, the stiffness and dampening characteristics of a particular “friction system” significantly impact the measured performance. When considering the environmental impact on friction performance, humidity and the presence of other chemical species (e. g. deicing agents, lubricants, and hydraulic fluids) play crucial role [14] [24]. Small-scale tester could easily accommodate the additional requirements, offer considerably larger flexibility and more accurate sensing/measurement of relevant parameters when compared to the full-scale friction and field tests. Nonetheless, there is no a standardized test procedure which could be applied to all the different small scale (subscale) testers, as it is hard to provide a universal testing procedure when friction performance shall be assessed [6] [25].



This thesis/research addresses adopts scaling philosophy and addresses brake performance due to interaction of nanomodified friction brake materials with external conditions. A pin on disk test setup is used to study the friction and NVH characteristics using triaxial accelerometer and microphone in the presence of varying relative humidity. Fast Fourier Transform (FFT) analysis is performed on the extracted data and the critical frequencies of vibrations are identified at different relative humidity. These high amplitude vibrations correspond to friction instabilities and influence the brake performance. The development of new testing strategy and procedures based in scientific principles and understanding of physical and chemical phenomena controlling friction will also be addressed.

## CHAPTER 2

### LITERATURE REVIEW

Friction is observed in our daily applications, in which automotive braking is observed frequently. In a typical friction brake, two brake pads or shoes are pressed against a rotor, to restrict movement between disc and pad surfaces, as shown in Fig 1. In this process, both the brake pads and rotor are subjected to wear. The friction behavior is determined by the system, by the character of the active surfaces of the rotor and pad friction called friction layer [26].

In 1490's, Leonardo da Vinci observed an increase in frictional force by increasing the normal force on the block [27]. In 17<sup>th</sup> century, French physicist Amontons published his work on friction. According to Amontons, friction is caused by surface roughness and the surfaces in contact have peaks and valleys, in which peaks of one surface lay in valleys of adjoining surface. He believed that the force which is required to pull the peaks up the other surface, until they clear. Amonton's mathematically formulated friction relationship as:

$$\mu = F_L / F_N$$

where  $\mu$  is the coefficient of friction,  $F_N$  is the normal force and  $F_L$  is friction force.

As shown in Fig.1, a block is dragged from left to right, a frictional force  $F_L$  acts against the dragging force. One must study the surface properties, to understand why friction force is

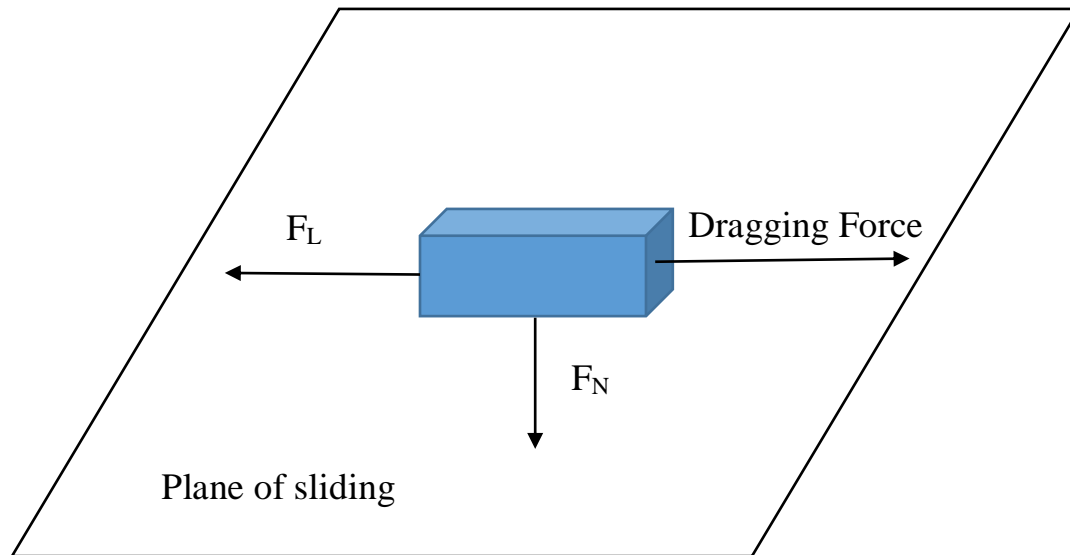


Figure 2 Illustration of Friction force

independent of normal contact area. In microscopic view all surfaces which are smooth also have a roughness value. According to Bowden and Tabor, when two solids are in contact, the upper surface is supported by the tips of the irregularities between the two solids [28]. When two rough surfaces are pressed against each other, the real contact area is very small. According to Jacobson and Hogmark, the real area of contact between two surfaces is defined by the hardness of two materials and applied normal load [29].

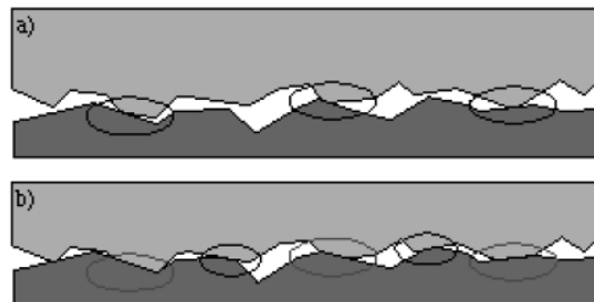


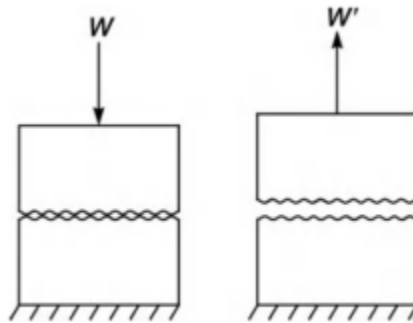
Figure 3. Contact situation between two rough surfaces.

a) Low load and/or high hardness b) High load and/or low hardness

Figure 2 shows that only few parts of the surfaces are in real contact with each other. With increase of normal load and decrease of hardness of the materials in contact, the real contact area between the two surfaces increases. Based on their research Eriksson and Jacobson [30] introduced the disc brake contact situation process theoretically. Initially primary plateaus are formed by abrasive particles present in the brake pads with regards to the third-body abrasion generated by wear debris [31]. The wear debris piles up against the primary plateaus and by applying normal pressure, shear forces and heat developed during friction, compacts the piled-up wear debris in forming secondary plateaus. The investigation done by Osterle and Bettge (2001) contradicted the characterization of contacting surfaces in the form of plateaus protruding from the surface by Eriksson and Jacobson [30]. On the other hand, they agreed on the point that a lower roughness is observed on the contacting surfaces when compared to the surrounding area.

It is believed that stick-slip causes high intensity and low-frequency noise [32]. Stick-slip phenomena occurs when static friction is higher than kinetic friction. In the case of automotive brakes, the stick-slip is depended on the friction material characteristics [33]. Yoon [34] investigated the propensity to generate stick-slip condition in brake system, he concluded that stick-slip increased with applied load and decreased with speed. Jang's [35] results show that by adding cashew and phenolic resin reduces the difference in coefficient of friction ( $\Delta\mu$ ), in case of brakes containing organic components. By decreasing the difference ( $\Delta\mu$ ) it is possible to reduce stick-slip [35]. In a braking system, vibration is being affecting by higher friction levels and negative friction-velocity slope which occurs at high humidity levels and low temperature. In addition, stick-slip phenomena are also affected by friction-velocity ratio ( $\mu$ -v) [35]. In a braking system, vibration can be reduced by minimizing the factors that cause stick-slip phenomena, which include properties of friction materials, speed, temperature and humidity [36].

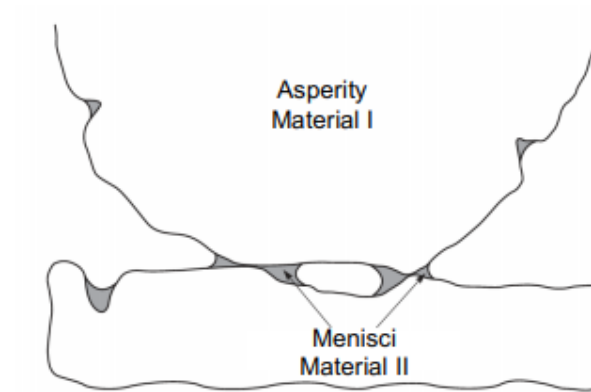
J. J. Bikerman [37] reviewed the importance of adhesion between the slider and the counter facing support in frictional phenomena. Adhesion is the phenomenon that occurs when two surfaces are in contact (either under a pure normal force or under combined normal and shear forces). According to Goryacheva and Makhovskaya, [38] adhesion is caused by molecular forces between the surfaces and significantly influences the characteristics of contact interaction of solids both in static contact as well as in sliding/rolling friction, particularly on micro- and nanometer scale levels. When two solid surfaces are clean, i.e when there are no contaminants present on the surface, the adhesive forces are stronger. On the other hand, in the presence of contaminants and at well lubricated conditions adhesion can decrease considerably [39].



*Figure 4 Schematic illustration of a normal force  $W$ , which forms an adhesive force and a tensile force  $W'$  which pulls to separate them [39]*

Earlier, several studies showed that the existence of nanoscale as well as microscale roughness is known to dramatically reduce adhesion between two contacting bodies due to a decrease in the real area of contact and increase the distance between bulk surfaces and only small area are in real contact [40] [41]. When two surfaces are in contact and asperities are close enough, van der Waals forces act between them. Surface roughness has an impact on adhesion

and friction, higher the roughness of the surfaces lower the real contact area is, which indeed lowers adhesion [39].



*Figure 5 Formation of menisci due to condensation of liquid molecules [39]*

Menisci are formed around the contact area, due to the condensation of liquid molecules around the asperities. These menisci alter the friction level and adhesion during sliding.

Depending upon the liquid level, menisci would increase or decrease the level of friction. From a liquid mediated contact, an external force which is greater than the meniscus force is required to separate both surfaces [39].

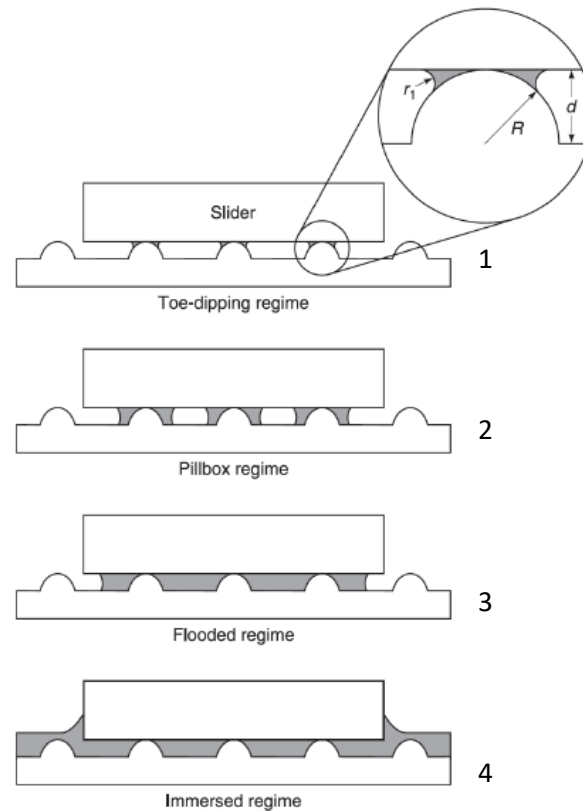


Figure 6 Regimes of different liquid levels [39]

Figure 5 illustrates a contact model of a slider on a rough surface with different regimes, varying in dependence on the present liquid levels. Menisci are formed in the first three regimes which contribute to meniscus forces. The first and third are the minimum and extreme regimes in which a small quantity of liquid condensate around the tips of contacting asperities or the entire surface [39]. The interface is fully immersed in the present liquid in the case of the fourth regime and low meniscus forces are observed when compared to other regimes. The tow dipping regime is directly proportional to normal load and is independent of apparent contact area [39]. The effect of water vapor or moisture influence on COF is observed by examining the effect of humidity. It is known that many brakes develop “morning sickness” which occurs during startup after overnight parking in between fall and spring when humidity could rise overnight and reach

a high level of 90% in cold morning [42]. It has been reported that friction associated with adsorbed water film and high humidity could be 50% higher than “dry COF” [43, 44]. As humidity increases, COF may have larger variation during initial sliding process which is related to surface tension [42]. When there is insufficient amount of water present between rotor and brake pad, the water film can fractionate into small bridges and surface tension of water at menisci [42]. High humidity could develop high friction due to capillary adhesive force for the interface with all surface and higher in case of smooth surfaces when water meniscus is substantially established [42].

Typically, a commercial brake pad consists of 1-8 vol% abrasive with a size of several microns [45]. Tribological characteristics of friction material are being influenced by a large number of particles in the form of oxides and carbides with varying size and shape [46, 47]. Use of inorganic fillers in polymeric composites is increasing, they alter friction performance, wear resistance and meet required performance. Some of the main advantages of nanoparticles: Firstly, nanoparticles exhibit large specific surface area which increases the propensity to transfer stress from matrix to nanoparticles and increases strength of composites, their hardness and wear resistance [48, 49]. Secondly, addition of nanoparticles helps in retaining the intrinsic merits of pure polymers. Thirdly, angularity of the abrasives is decreased with decreased particle size which leads to the improvement of mechanical behavior of the polymer [50]. It has been demonstrated that to achieve the optimal friction performance, the polymer matrix composites should be modified with different materials [45].

Wang [51] summarized the effects of nanoadditives on polymeric matrices and concluded that by adding nano-fillers to polymers not only can lead to an increase of the friction performance, but it can also decrease it, and nanoadditives alter friction performance in different



ways. Friction performance is typically judged by the level and stability of the COF, wear rate, propensity to vibrational and noise and environmental aspects. Lee [52] studied different abrasives including zirconia, quartz,  $\text{Fe}_2\text{O}_3$ ,  $\text{Fe}_3\text{O}_4$ , MgO and SiC with different sizes 1 and 150  $\mu\text{m}$  and concluded that size was one of the dominant factors in controlling friction oscillations and stability. J. Bijwe [53] worked on 3 different abrasives in nano and micron sizes for developing friction materials and concluded that all performance parameters were significantly affected due to nano-fillers as they form thin coherent film on both the surfaces in case of NCs which is responsible for enhanced friction performance. According to Li [54] lubricating oil with  $\text{ZrO}_2$  and  $\text{SiO}_2$  nanoadditives and decrease in average coefficient of friction as the nanoparticles were eventually transferred to the friction contact and altered sliding friction into rolling friction.

Hence, the formulation of brake pads plays a vital role in friction behavior. According to Osterle [55] the relationship between composition and property of friction materials is not known well enough, the formulation is based on trial and error and thus is expensive and time consuming. Testing is another important thing which shows the effectiveness of an automotive brake [56]. Many brake manufacturing companies conduct laboratory tests using brake dynamometer. But to overcome the cost and time effectiveness in testing friction materials Bruker has developed a Universal Mechanical tester (UMT) which is a bench top tester and can test brake pads much efficiently than dyno [56].

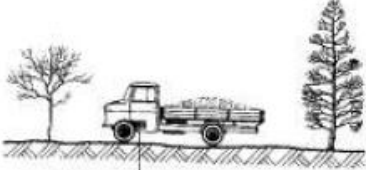
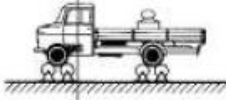

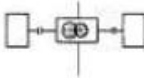
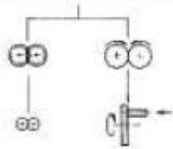
Category		Descriptive	Illustration
I	Performance testing on real test pieces	Field-test	
II		Simulation	
III		Large-scale tests with real aggregates or parts	
IV	Modelling of friction and wear mechanisms	Small-scale test with real aggregates or parts	
V		Standard tests on small-scale test specimen	
VI		Modelling	

Figure 7 Possibilities for scaling tribo testing

Figure 6 provides research done by Czichos, varying from on-field tests to laboratory testing with simple geometry [57] and concluded that in laboratory tests, the factors that determine wear rates are not sufficiently well controlled. Using chase type friction tester, Ertan and Yavuz [17] demonstrated that, manufacturing parameters influence the friction stability, wear resistance of pads rubbed against surface of gray cast iron rotor. Oliviero Giannini [58] conducted a research to characterize the vibration and noise. They designed and built a laboratory test model for controlling experimental studies of noise emission in automotive brake. Their results indicated that frequency of vibration is affected by the stiffness of caliper, but the vibration of the whole system remains qualitatively the same.

Many researchers compared large scale dynamometer and small-scale chase machine, but these tests were conducted without scaling methodology. A. Wahab et al [59] used the scaled down methodology to evaluate the thermal performance of disc brake. A comparison is done between full-scale dynamometer and bench top material screening tester to evaluate the performance of a brake pad and it is demonstrated that the scaled down tester is reliable, effective for screening tests and to evaluate brake pad friction performance [60]. The automotive industry uses inertia-dynamometer tester for screening tests, the main reasons for performing screening tests are to study the friction and wear properties of materials and to rank the materials. On small scale UMT features, low cost and less time for evaluation. Proper scaling methodology must be used to evaluate the wear and friction performance in the case of a small-scale bench top tester. There are different scaling laws depending on their involvement in the fields of applications [61]. Some of the scaling laws which are essential include the following.

#### Scaling:

Due to the increase in dependency of modern technology on miniaturization, scaling laws are used to predict the behavior of a larger system on a small-sized scale model. Some researchers call these laws by the name “dimensional analysis”. There are 2 types of scaling, isomorphic and allometric. In case of isomorphic scaling, all the aspects of a device scale with respect to geometric integrity. When different aspects scale in different ways, it is called “allometric” scaling. In miniaturization scaling laws play a vital role in understanding different physical aspects involved in complex systems. All quantities in physics have dimensions that can be expressed in fundamental quantities they are mass (M), length (L) and time (T). Scaling of different geometric parameters follows the laws given below

## Scaling of Area and Volume

The general rule is called “square law”:

$$(\text{ratio of areas}) = (\text{ratio of lengths})^2$$

$$(\text{ratio of volumes}) = (\text{ratio of lengths})^3$$

These two relationships can be expressed in one governing equation [62]:

$$(\text{ratio of volumes})^{(1/3)} = (\text{ratio of areas})^{(1/2)} = (\text{ratio of lengths})^1$$

Consider a simple rectangular solid, with length  $l$ , height  $h$  and thickness  $t$ . Each of these dimensions can be generalized as a characteristic dimension “ $l$ ”. Different quantities can be expressed (characterized) by the initial characteristic length  $l$ . For instance, mass is equal to density times volume ( $m = \rho V$ ). Density is constant, as we are scaling for the same material and density is a material property. So that mass is directly proportional to volume, which in turn is expressed by the third power of characteristic length. Therefore,

$$m \propto l^3$$

Volume is expressed using the characteristic, length  $l$  as follows

$$V = htl \propto l \cdot l \cdot l \propto l^3$$

So, volume is expressed as the third power of characteristic length. In similar way the surface area is expressed by the second power of the characteristic length

$$S = 2(ht + tl + hl) = 2(l^2 + l^2 + l^2) \propto l^2$$

In case of force, we all know that

Mechanical Force ( $F$ ) =  $mg$ , where  $g$  is gravitational constant

$$F = mg \propto l^3 \text{ (Mass is always proportional to the volume of the body)}$$

So, force is expressed as the third power of characteristic length. In similar way the acceleration is expressed by the zero power of the characteristic length

From the second law of motion,  $F = ma$  or  $a = F/m$

$$a = l^3 / l^3 = l^0 = 1$$

In case of surface to volume ratio is expressed by the power of negative one of the characteristic length.

$$S/V = l^2 / l^3 \propto 1/l$$

In order to scale time, the displacement equation can be used:

$$S = (1/2).a.t^2,$$

where

a is acceleration, S is displacement, and t is time Hence,

$$t = (2 S/a)^{1/2} = (2 Sm/F)^{1/2}$$

By substituting the scaling of mass and force, we have:

$$[t] = [s]^{1/2}[m]^{1/2}[F]^{-1/2} = [l]^{1/2}[l^3]^{1/2}[l^3]^{-1/2} = [l]^{1/2}$$

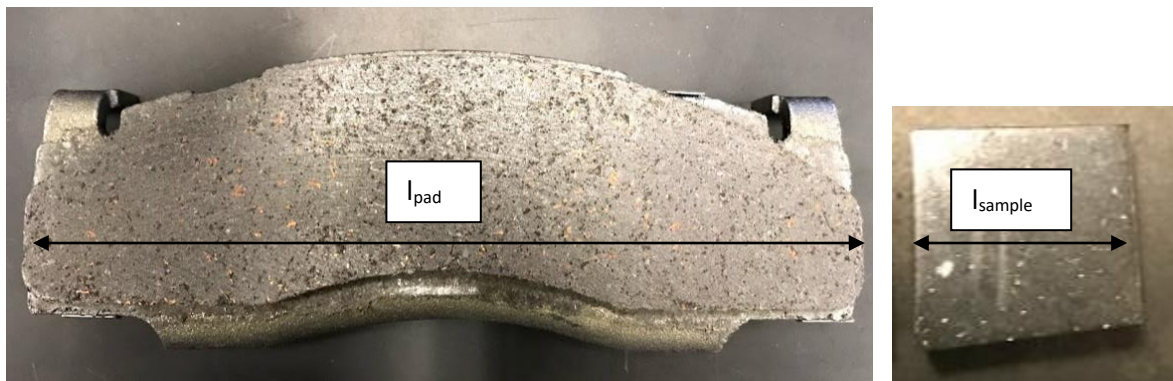


Figure 8 length comparison of real brake pad to pad sample

Figure 8. shows real brake pad and pad sample, where  $l_{\text{pad}}$  is length of real brake pad and  $l_{\text{sample}}$  is length of cut down sample. In this thesis, scaling is done based on area, let  $A_1$  be area of real brake pad and  $A_2$  be area of cut down pad sample and consider  $S$  as scaling factor.

We know that area of the pads and samples are being used to scale down the results:

$$(\text{ratio of areas}) = (\text{ratio of lengths})^2$$

Hence,

$$\frac{\text{Length of real brake pad}}{\text{length of pad sample}} = S$$

$$\text{Ratio of areas} = \frac{\text{Area of real brake pad}}{\text{Area of pad sample}} = \left( \frac{\text{Length of real brake pad}}{\text{length of pad sample}} \right)^2 = S^2$$

Similarly, other parameters with their scaling factor are given in table. 1

Table 1. Scaling in different parameters

<b>Parameters</b>	<b>Scaling factor for parameter</b>
<b>Force(N)</b>	$S^3$
<b>Velocity (meter/sec)</b>	$S^{0.5}$
<b>Time (sec)</b>	$S^{0.5}$
<b>Angular velocity (rpm)</b>	$S^{-0.5}$
<b>Energy(J)</b>	$S^4$

In current testing, Universal Mechanical Tester will be considered as small-scale test and scaled down parameters are calculated for different braking scenarios. In the current thesis, the following parameters which include Normal load, pressure, rotational speed of disc, acceleration and time were scaled down and are determined for Universal Mechanical Tester using the real braking test and drag test scenarios. These tests are conducted for same materials but at different humidity levels and then a comparison is done between different testing conditions. Friction induced vibrations is also addressed as it is one of the factors which determines the brake performance.

## **CHAPTER 3**

### **STATEMENT OF OBJECTIVES**

1. Demonstrate the effect of humidity in nano-modified brake pad materials when subjected to different humidity levels.
2. Explore differences obtained with different braking conditions which include, real braking and drag test testing scenarios.
3. Correlate the friction induced vibration to detected friction levels and stability and to generated noise.



## CHAPTER 4

### EXPERIMENTAL

#### 4.1. Brake pad model samples

The experiments described in this paper are conducted on two model brake samples prepared in laboratories. Composition of these model samples was based on a series of materials used for manufacturing commercial brakes. Different types of commercial brake pads are available in US, classified as semi-metallic (SM), Low-metallic (LM), non-asbestos organic (NAO) [1]. Modified phenolic resin, polymeric fibres, ceramics, nano additives  $ZrSiO_4$  (50 nm average size), metal compounds and solid lubricants were weighted with accuracy of  $\pm 1$  mg (OHAUS Explorer Pro balance), mixed in Stephan vertical mixer (model 2786) for 12 minutes, hot pressed in a cylindrical steel mold (inner diameter of 50mm) at 20 MPa and 170°C for 15 minutes and subsequently post cured in programmable furnace (Isotemp, Fisher Scientific) at 180°C for 4 hours. Friction samples with dimensions of 10 X 10 X 7 mm and density varying between 2.3 (NAO) and 3 gm/cc (LM) were cut-off by using water cooled precision diamond saw (Buehler, ISOMET 4000).

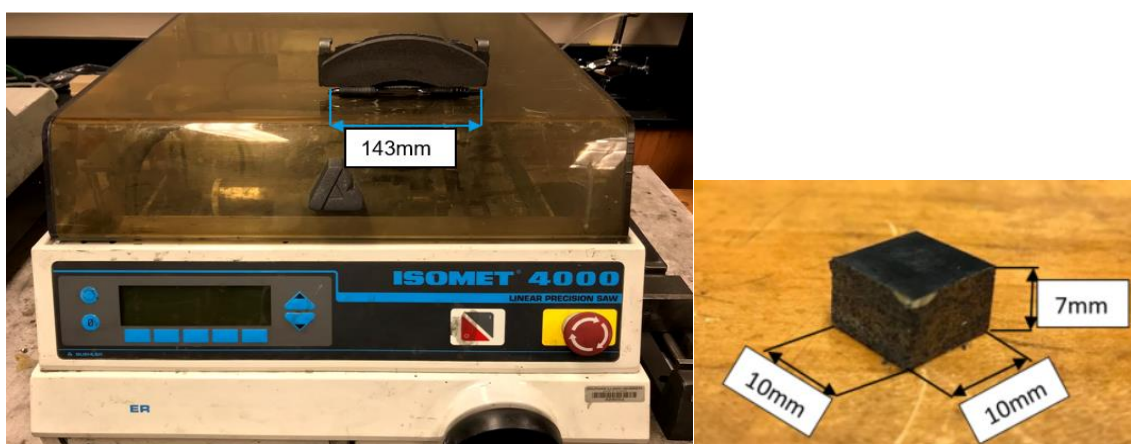


Figure 9 (a) Buehler ISOMET 4000 and (b) Sample used in holder

#### 4.2. Rotor material

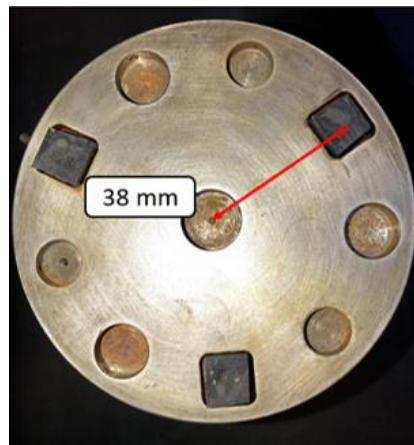
The rotor used is a grey pearlitic cast iron which is typically seen in passenger vehicles. The diameter of rotor is 97 mm and its thickness is 12 mm as shown in Figure 2. Surfaces of cast iron rotors were prepared by grinding using a BUEHLER sand paper with 320/P400 grid and the tested friction couple were subjected to run-in procedure before testing [1].



*Figure 10 Pearlitic cast iron rotor*

#### 4.3. Sample holder

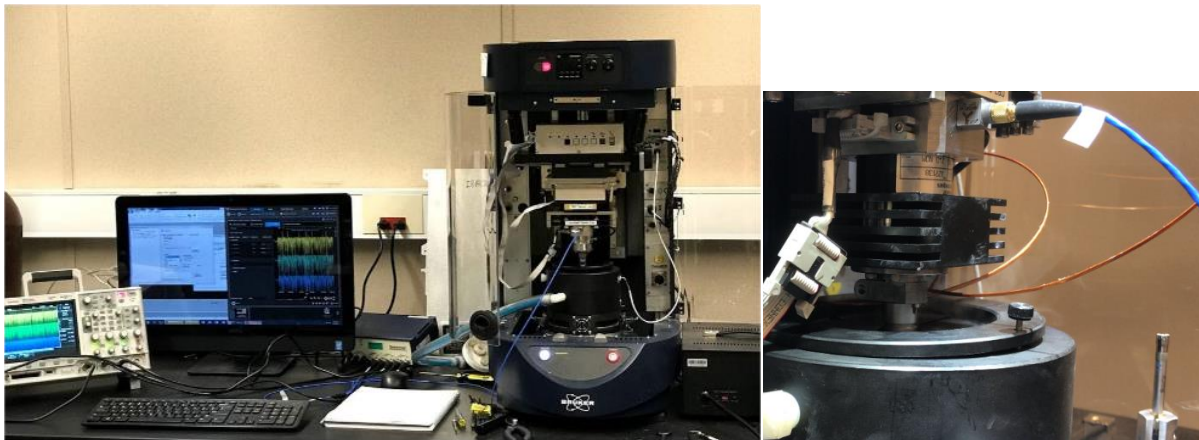
A sample holder is designed in such a way that it can fit inside the humidity chamber and is used to hold the three samples at a radius of 38mm is used as shown in Figure 3



*Figure 11 Sample holder used in UMT*

#### 4.4. Universal Mechanical tester (UMT)

Bruker's brake Material Screening Tester for the UMT Tribo Lab was specifically developed to be a cost-effective, fast screening and rank materials before performing the component level evaluation, with the techniques used, the tribological performance of small, friction material samples can be characterized in a precise and timely manner, while mounting key parameters such as sliding speed, friction, wear, vibration and temperature [2]. Universal Mechanical tester with a humidity chamber is shown in below Figure 4. The humidity chamber which is controlled by the humidity generator is being isolated from the outer environment. Both UMT and the humidity chamber were operated form a computer.



(a)

(b)

Figure 12 (a) UMT Bench Top Tester (b) Accelerometer and microphone mounting.

A force and torque sensor are equipped on this sub scale tester to monitor the normal load applied and the torque generated by the friction pads. The force sensor can measure up to 1000N of load with accuracy of  $\pm 0.01$  N and torque sensor can measure up to 30Nm with an accuracy of  $\pm 0.01$  Nm. A closed chamber with enough space to accommodate the sample holder and rotor is used to maintain the humidity level. The chamber has an inlet connected to a humidity

generator by means of a hose pipe which allows dry and wet air to flow into the chamber. The humidity generator can generate relative humidity of up to 90% with an accuracy of  $\pm 0.1\%$  and the humidity level is monitored by the means of a sensor placed inside the chamber.

Vibration response was monitored by tri-axial ICP accelerometer (PCB Piezotronics, Model=356A45) coupled with Oscilloscope (Agilent Technologies, Model=MSOX2024A), this accelerometer is capable of measuring frequency between 0.8 and 8000 Hz. Noise response was monitored by a 1/4" free-field, prepolarized microphone (PCB Peizotronics, Model==377C01) which can measure between a range of 4 and 100 KHz. The accelerometer is mounted on the machine as shown in Figure 6, which is nearer to the sample holder using adhesive mount and the microphone is stuck on to the platform around the chamber to recover every sensitive sound occurring. Keysight BenchVue software is used to save data from the oscilloscope at a sampling rate of 50 KHz. Data from the sub scale tester is extracted at a sampling rate of 18KHz using UMT Viewer software (Bruker).

#### 4.5. Run-in Process

Run-in ensures that pad samples touch the rotor evenly and with a largest possible contact area. Typically, automotive dynamometer tests standards require that at least 80% of the apparent pad contact area “touches” the rotor counter face. Initially after grinding the rotor with sandpaper, a 180-grid sandpaper is stick on the surface of the rotor. The cut down samples are placed in the sample holder and then a load of  $F_z = 200$  N is applied for 5 minutes, followed by a relaxing time of one minute to prevent samples from being overheated. Five periods were performed as shown in Figure 5. After run-in process, friction force approached to converged values in the end after five periods as shown in figure 6, it meant that the samples and the rotor were evenly touched, and the following tests were trustworthy.

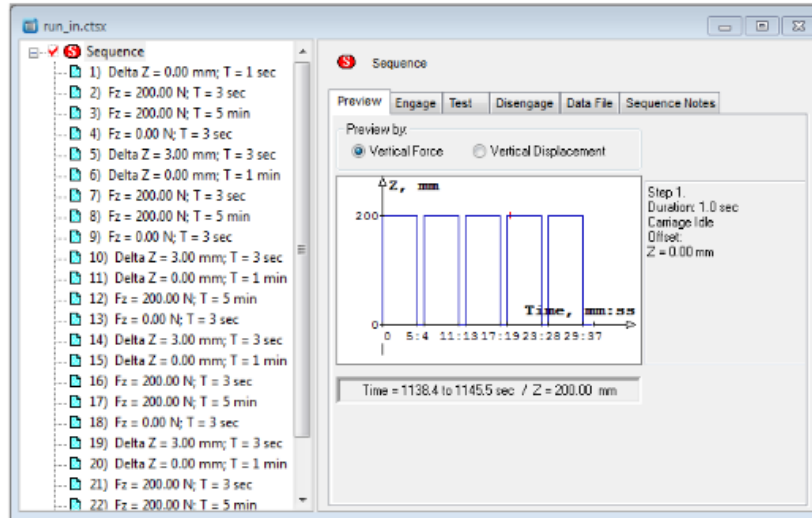


Figure 13 Run in process

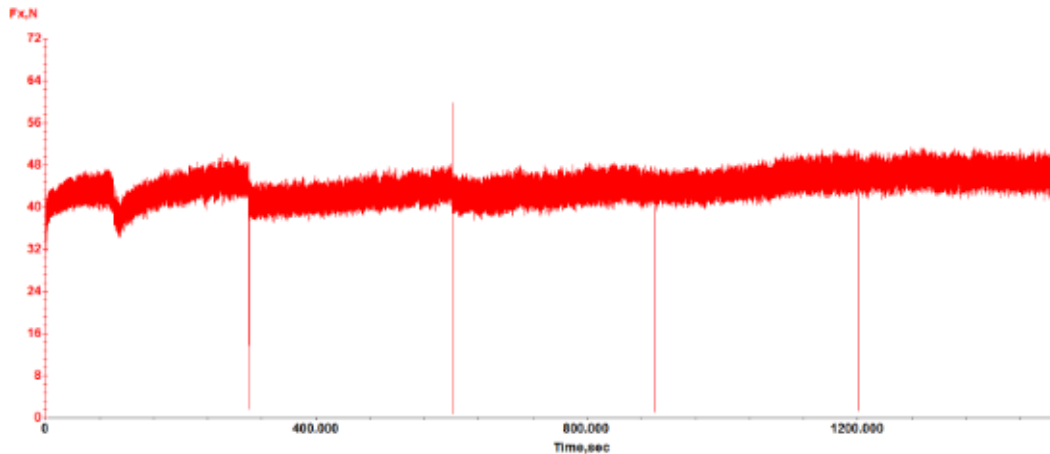


Figure 14 Friction force during Run in process

#### 4.6. Friction Test Scenarios:

Two brake test scenarios were performed at different humidity levels. The first test is real braking simulation test, which is a parking lot scenario in which the car starts braking from 5 Mph to rest, during this process the braking load increases from 0 to 300N correspondingly. In real braking simulation testing, both the applied load and speed varies. The second test is drag test it is assumed that car is moving at 5 Mph with a load of 300N applied constantly throughout

the test. Both the tests are conducted at extreme humidity levels with 15% RH as lower humidity level and 65% RH as higher humidity level.

Each model brake is tested for 3 repetitions and the average of the three tests are reported. Data from accelerometer and microphone are extracted using oscilloscope and Keysight BenchVue software during steps 3 & 5. The data from oscilloscope are collected at a sampling rate of 50KHz and from sub scale tester at a sampling rate of 18 KHz.

Fast Fourier Transform analysis was used to analyze data obtained from the sub scale tester and oscilloscope to convert the mechanical vibrations and coefficient of friction oscillations signal into amplitude and frequency. Matlab (Mathworks, Version=R2015a) was used to perform Discrete FFT analysis on the data obtained at a sampling rate of 18KHz for better data comparison.

#### 4.8. Surface analysis:

Friction surface analysis was performed after friction test. Friction surface of tested samples was investigated by using Scanning Electron Microscopy (SEM), which is a technique used to produce images by scanning the surface with a focused electron beam. The topography of the surface is created by scanning the sample and collecting the secondary electrons which are collected by special detector. The samples surfaces were observed after running friction tests at 20%RH and 70%RH for both the braking scenarios.

## CHAPTER 5

### RESULTS AND DISCUSSION

#### Friction Tests:

Real brake simulation and drag tests are conducted at different humidity levels in UMT. Then, by using MATLAB graphs are plotted and put together for easier comparison. In the following graphs, the blue line indicates COF at higher humidity level (65%RH) and black line represent COF at lower humidity level (15%RH).

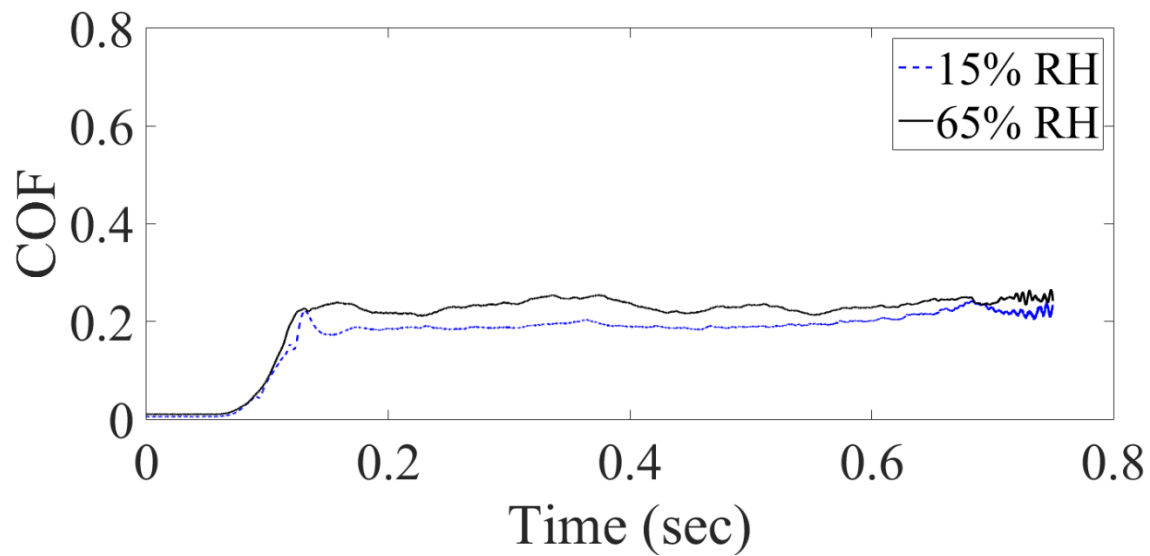


Figure 15 Real Braking test for Model material 1 (LM)

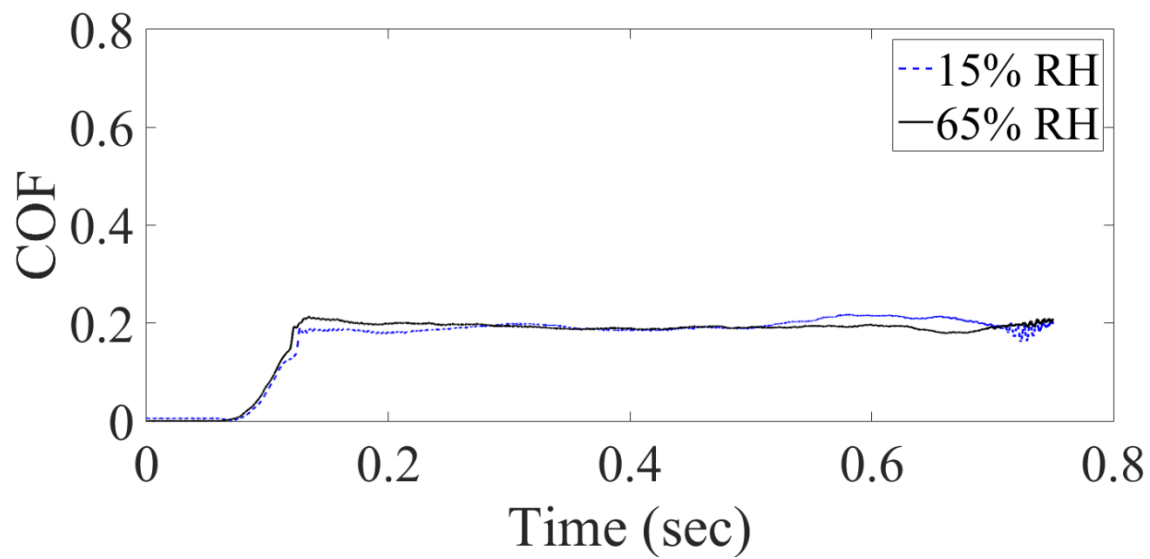


Figure 16 Real Braking test for Model material 2(NAO)

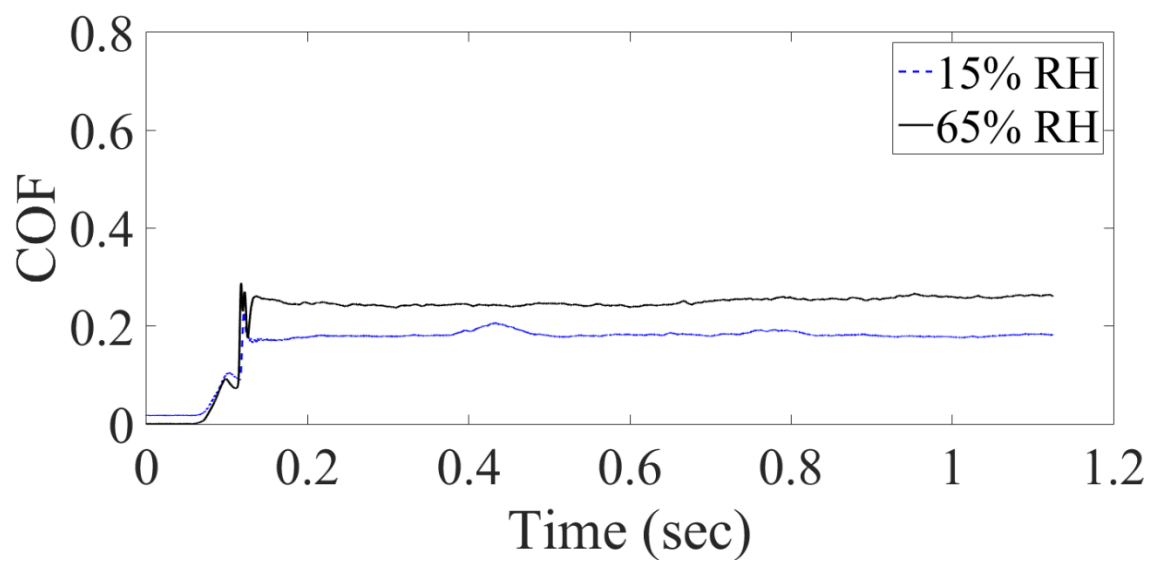


Figure 17 Drag test for Model material 1 (LM)



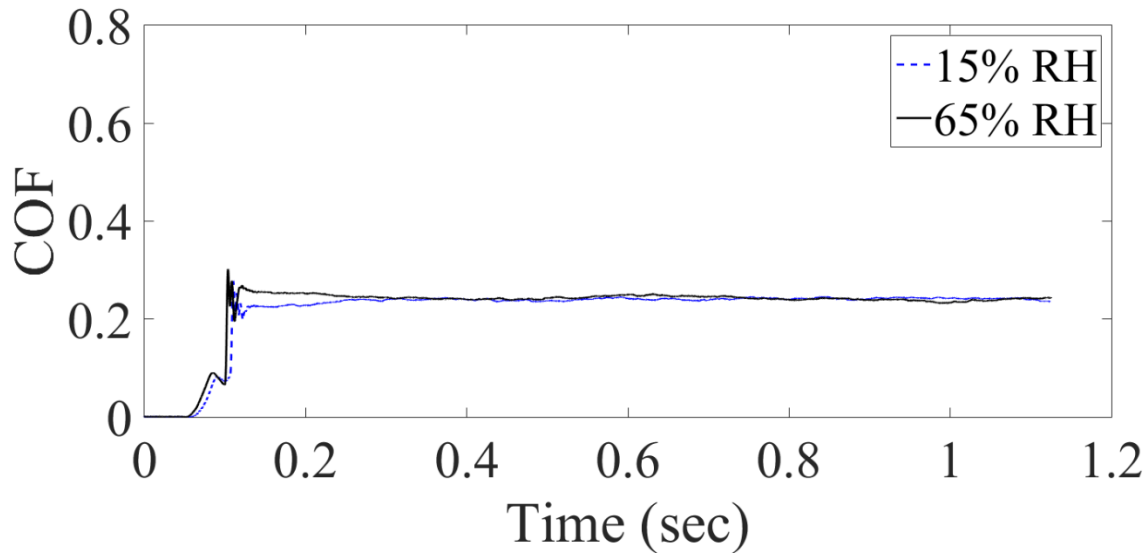


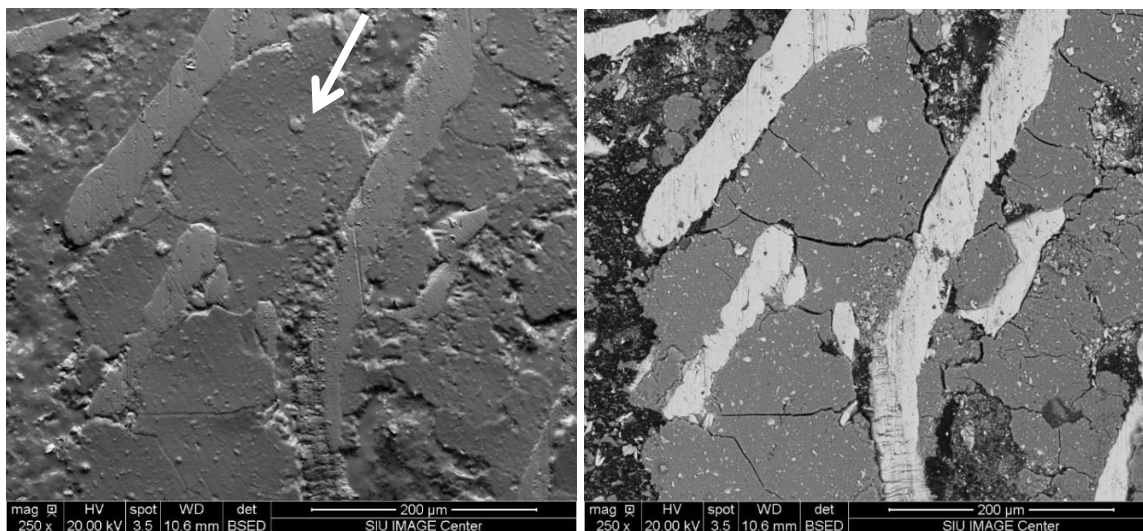
Figure 18 Drag Test for Model material 2 (NAO)

Figures 15, 16, 17 and 18 show the detected COF for two different samples tested at different humidity's, for 2 different Friction tests. In case of real braking test, friction coefficient is higher at 65%RH when compared to the values detected at 15%RH for modal material 1(LM) (figure 15). Although, this increase of the COF with increased humidity level contradicts with the observation by [21]. In figure 16 COF is initially higher for model brake 2 (NAO) but, tends to decrease in the end. COF is unstable for LM at different humidity levels when compared to NAO. On the other hand, for drag test COF is stable in different humidity levels for both LM and NAO. In figure 10 NAO has almost equal COF at 15%RH and 65%RH, this shows that humidity does not affect the friction performance of NAO brake pad. In all the cases, the difference between COF at 15%RH and 65%RH is higher for LM, than that of NAO. The average COF for NAO at 15RH is higher than that of LM. When comparing both the real braking and drag tests, it's clearly observed that COF is more stable in case of drag test (Figures 17 and 18).

Surface Analyses of tested Samples after Friction tests:

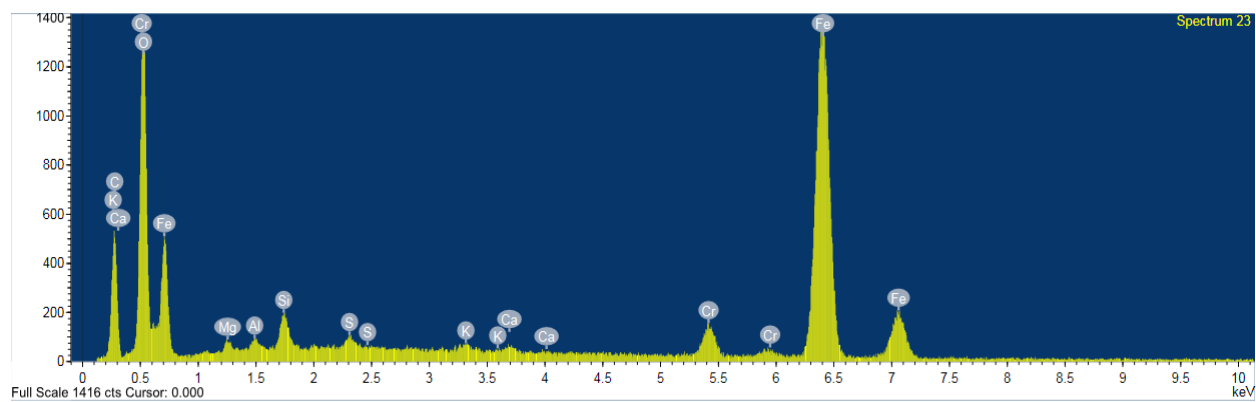
Friction surface of tested samples was investigated by using SEM equipped with the energy dispersive X-ray microanalysis. Figure 16 shows the characteristic topography of friction surface as observed in model pad material 1 (LM sample). The elevated plateaus are formed on metallic fibers present in brake pad composite. Obviously, the real contact area is considerably smaller than the apparent surfaces of pad samples. The contact is predominantly on the metallic chips, but there are few plateaus formed by compacted wear debris.

Model samples LM and NAO revealed their different chemistry. While LM contains metallic chips, NAO is formulated without metal fibers. The role of metallic fiber is to reinforce the composite and to increase its thermal conductivity, but it also impacts the contact area with the rubbing counter-face (gray cast iron). It is easily visible that the valleys surround the plateaus by removal of wear debris [35]. In figure 16 (b) the bright spots are visible as metallic chips or heavier compounds and the dark areas are related to rubber or coke. Several micro-cracks can be easily seen in Figure 16, they indicate that fatigue mechanism was also involved in sliding process. EDX analysis shown in Figure 16 (c) provide chemical components of friction surfaces as detected for modal material 1 after friction tests. Bright strips in Figure 16 (b) were associated with steel chips with typical grooving, indicating abrasive wear. Little amounts of Mo were also observed which could be due to transfer from wearing of cast iron rotor. A great amount of iron was detected, and iron oxide is the dominant component detected. Besides iron, Si was also present in this area. Si presence could be abrasive silicate particles like silicon dioxide ( $\text{SiO}_2$ ). The presence of Ca, Cr and K can be associated with potassium titanate ( $\text{K}_2\text{TiO}_3$ ), calcite ( $\text{CaCO}_3$ ) and calcium sulphate ( $\text{CaSO}_4$ ). Besides Fe and Si, it is noticed that presence of calcium was also dominated on the friction surface.



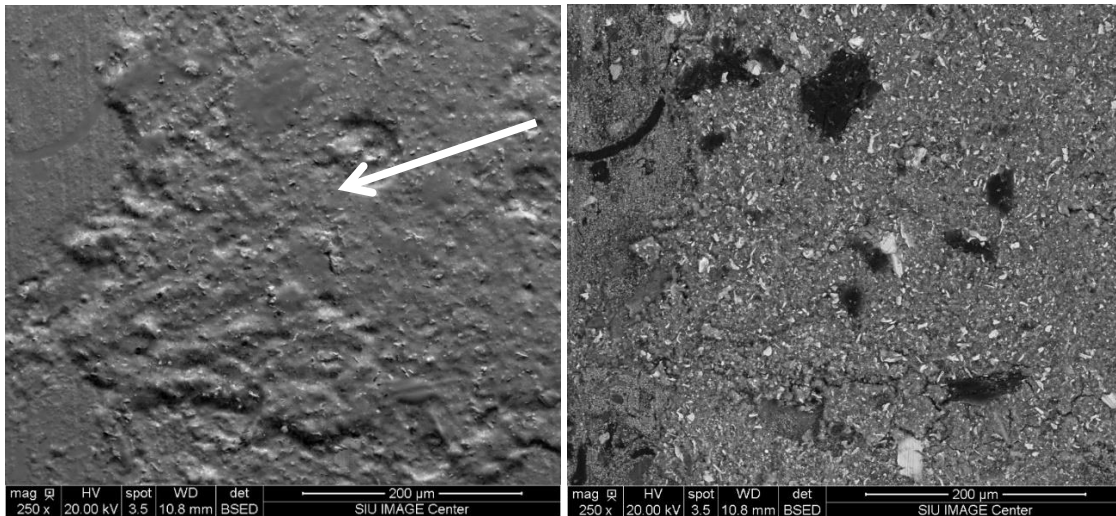
(a)

(b)



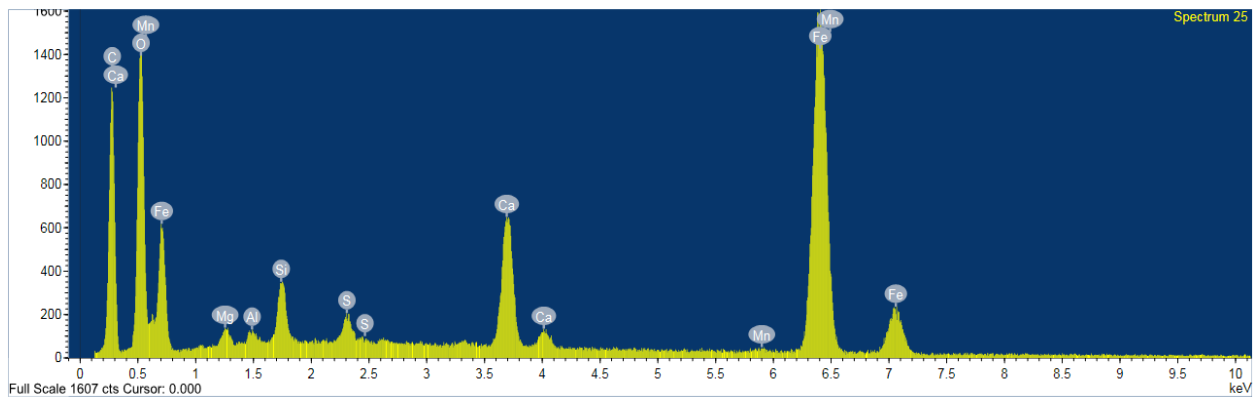
(c)

Figure 19 (a) SEM of modal material 1 at 250X magnification, (b) Back Scattered Electron image for modal material 1 and (c) EDX analysis of Modal material 1 after friction tests



(a)

(b)



(c)

Figure 20 (a) SEM of modal material 2 at 250X magnification, (b) Back Scattered Electron image for modal material 2 and  
(c) EDX analysis of Modal material 2 after friction tests

Figure 20 shows characteristic topography of friction surface as observed in modal material 2 (NAO) these images indicate that the surfaces included valleys (White arrows), and plateaus. The sliding directions are indicated by the grooves, which shows the evidence that abrasive particles remained after friction process. Friction layer formed during braking process plays a major role in determining friction performance. However, structures and chemical

components on the friction layer tremendously differ from the entire matrix [33]. A friction layer is generated on a friction surface after sliding process, and it is formed from wear debris by compaction and sintering at high temperatures [34]. Components from plateaus due to higher wear resistance and those wear debris result in flat surfaces [34]. From Figure 20 it is clearly observed that the contact area of modal material 2 is predominantly formed by a friction layer formed on the surface from captured wear debris. Figure 20 (c) represents EDX analysis of Modal material 2 after friction tests. Fe and Mn elements dominated this area and the existence of Si, Mg, Zr and Al are possibly related to Silicon dioxide ( $\text{SiO}_2$ ), Aluminum oxide ( $\text{Al}_2\text{O}_3$ ) and zirconium silicate ( $\text{ZrSiO}_4$ ) used in the formation of brake pads. Modal material 2 is NAO (Non-Asbestos Organic) brake pad which does not have any metallic elements in the brake, presence of iron results in the formation of friction film from the wear of iron present in brake disc which is gray cast iron. With the presence of oxygen, instead of pure metals, metal oxides such as aluminum oxide, iron oxide and magnesium oxide most likely existed. The surface chemistry of both the samples are compared and it is observed that chromium components are only present in LM material, from results we know that LM material, is having unstable COF, this instability might be occurring in LM due to the existence of chromium components in it.

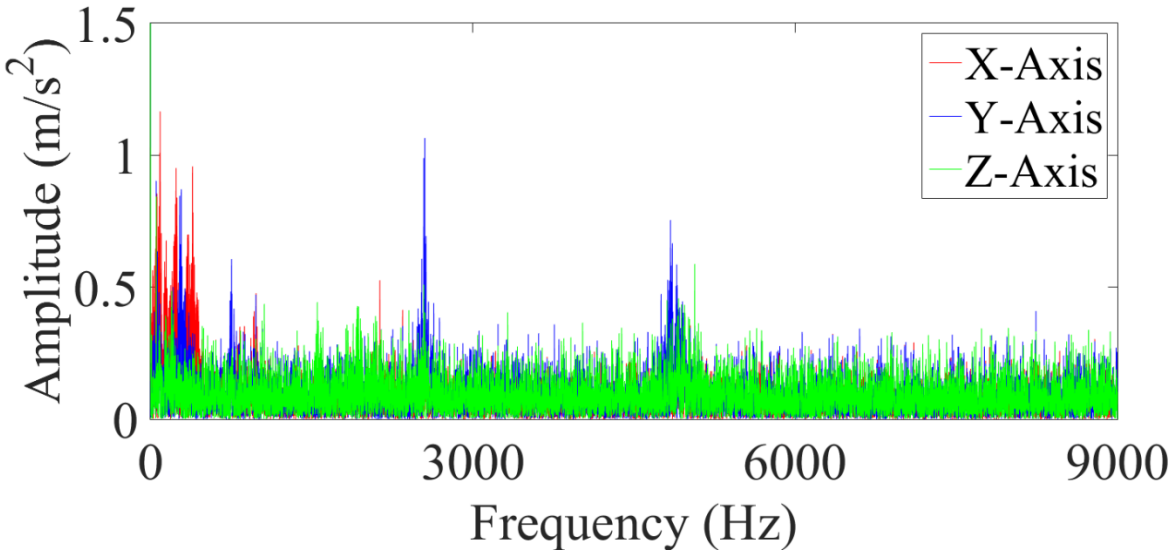
Friction induced vibration and noise:

Real braking test:

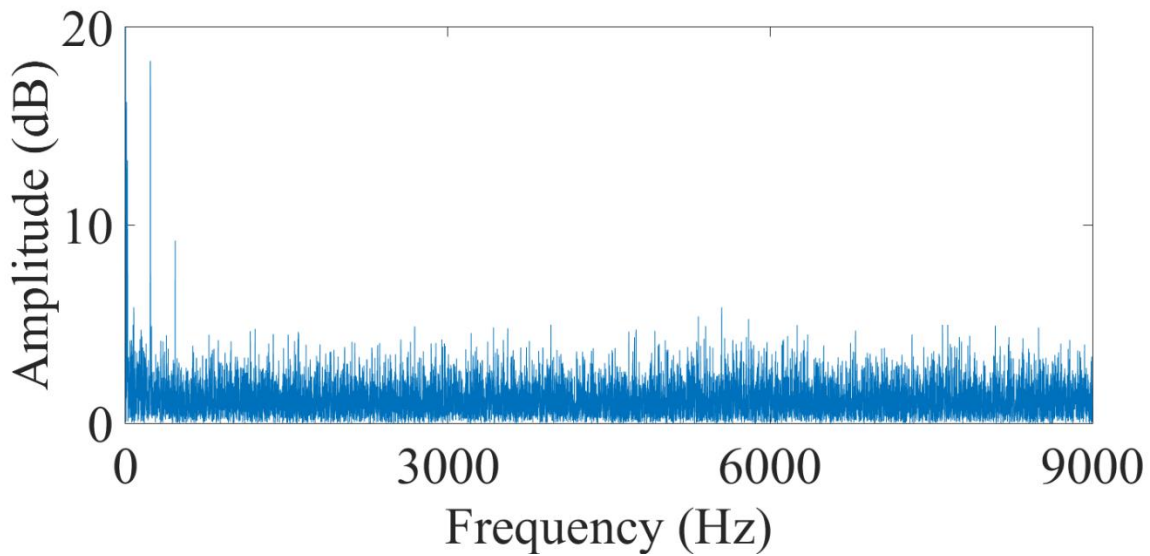
Figure 21 (a) represent the accelerometer vibrations, 21 (b) represent the noise recorded and 21 (c) represent the distribution of COF for modal material 1 at low humidity level.

Significant vibrations are observed initially during the engagement with an amplitude range of (0.5-1)  $\text{m/s}^2$ . Few peaks are observed at 3000Hz and 5000Hz frequency with an amplitude of 1  $\text{m/s}^2$  and 0.75  $\text{m/s}^2$  respectively. But, there is no noise recorded by the microphone at these peaks, microphone recorded data with amplitude near to 20dB in the initial stage, during the

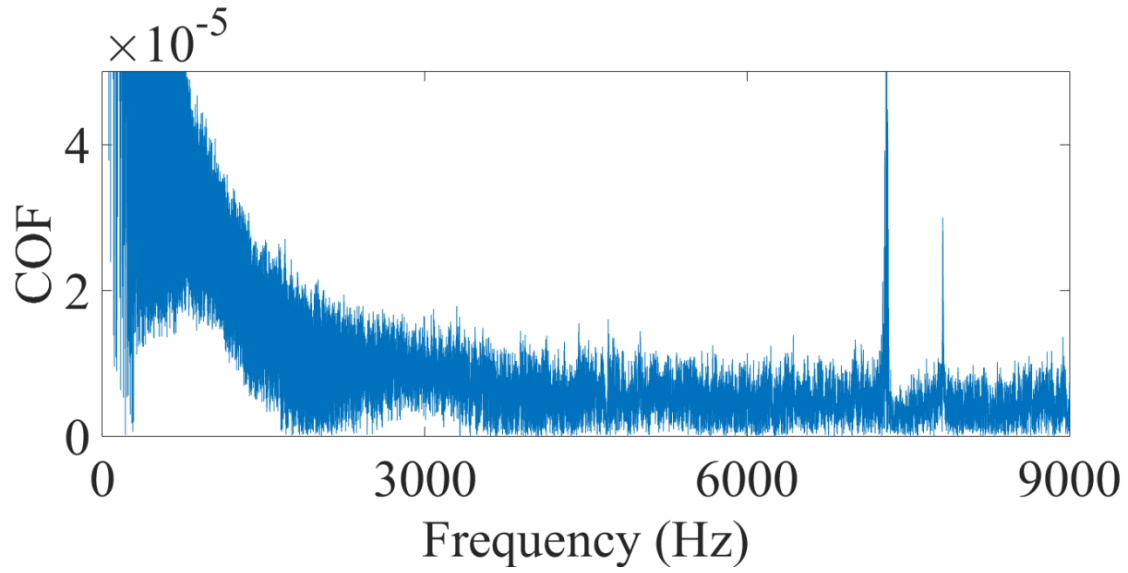
engagement of samples with the rotor. In between 6000Hz and 9000Hz frequency peaks are observed in recorded COF with amplitudes  $4 \times 10^{-5}$  and  $3 \times 10^{-5}$  respectively, but there is no noise dependence during these peaks, neither any vibrations are observed in the accelerometer.



(a)

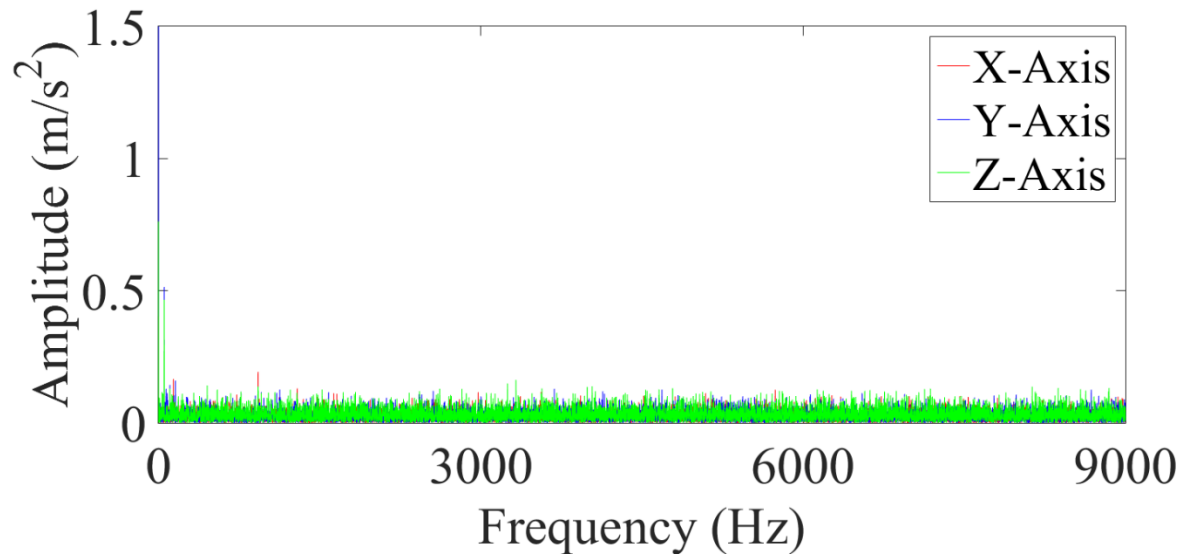


(b)

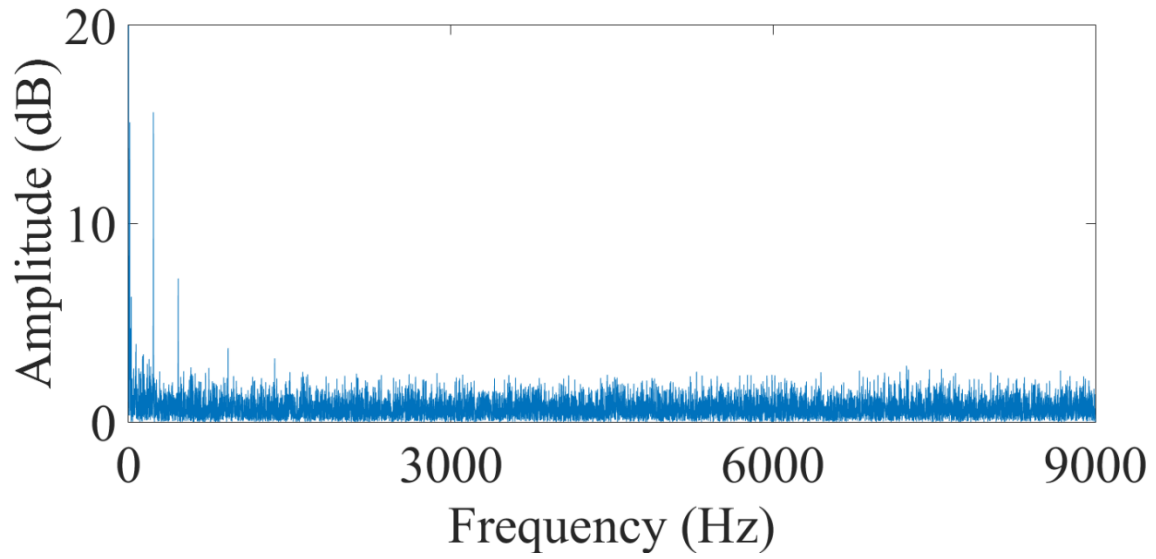


(c)

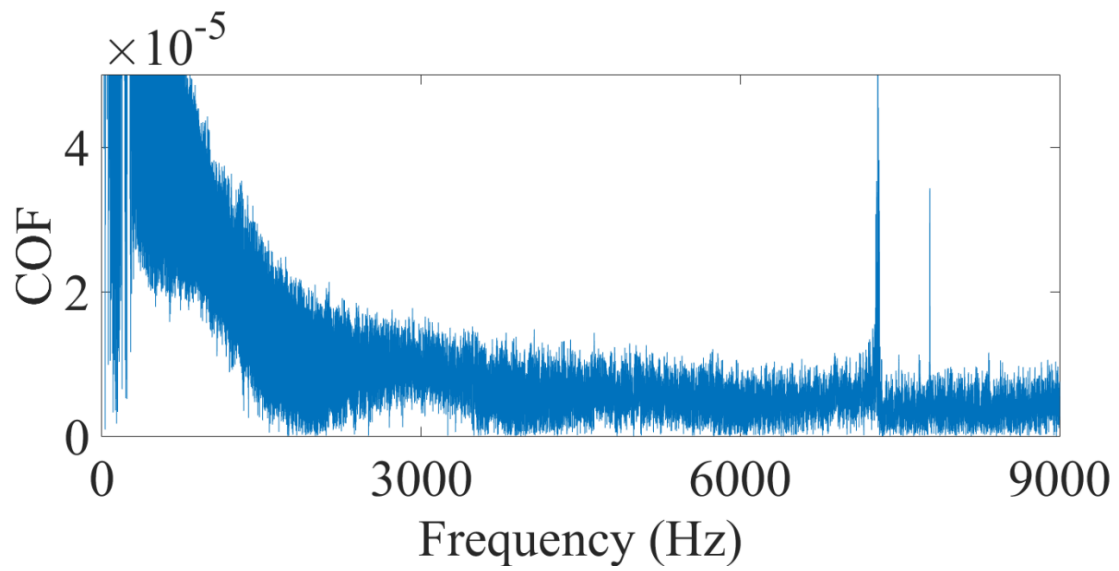
Figure 21 FFT analysis of accelerometer (a), microphone (b) and COF in UMT (c) for modal material 1 at 15%RH



(a)



(b)

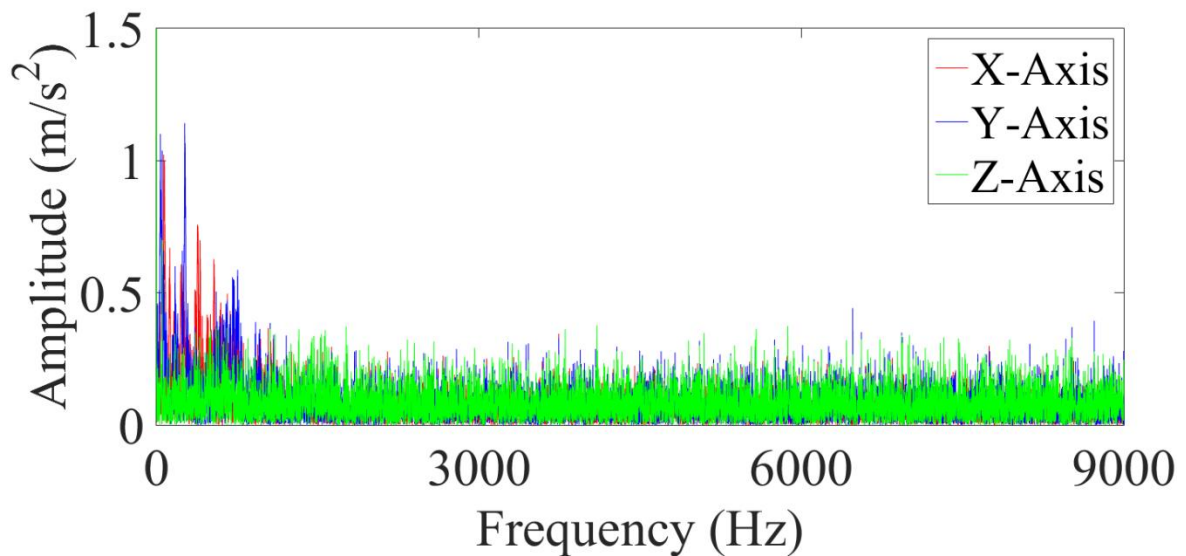


(c)

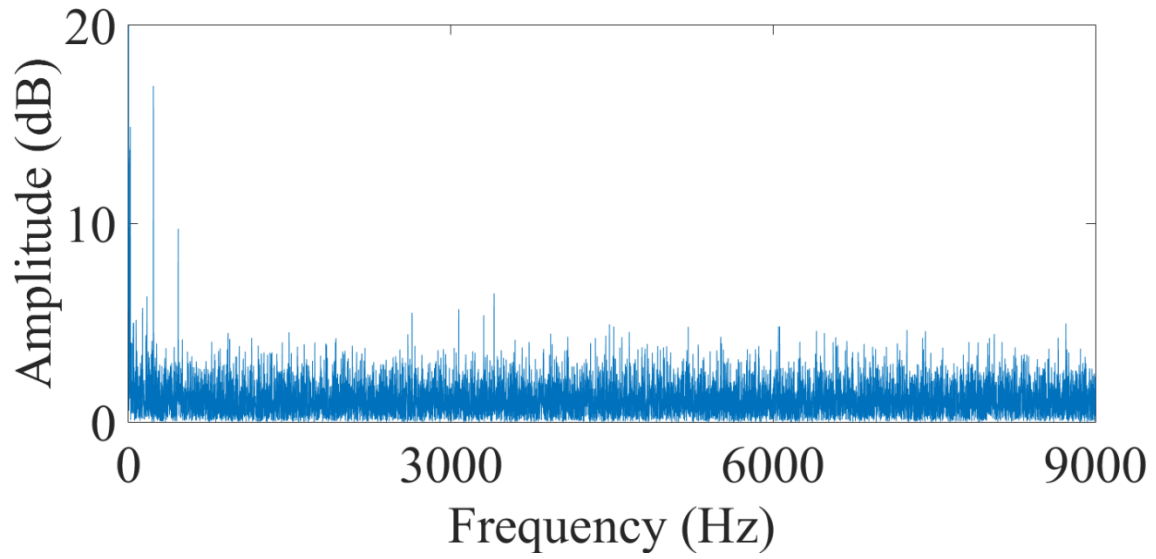
Figure 22 FFT analysis of accelerometer (a), microphone (b) and COF in UMT (c) for modal material 1 at 65%RH



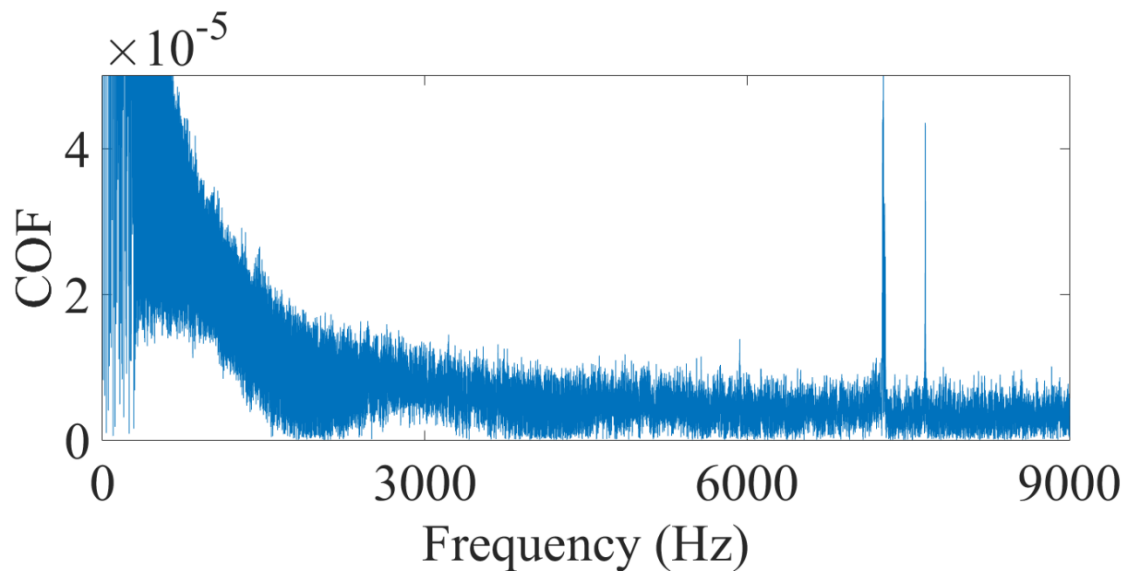
Figure 22 (a) represent the accelerometer vibrations, 22 (b) represent the noise recorded and 22 (c) represent the distribution of COF for modal material 1 at high humidity level. No significant vibrations are observed during the complete friction test. Microphone recorded data with amplitude near to 15 dB in the initial stage, during the engagement of samples with the rotor. In between 6000Hz and 9000Hz frequency peaks are observed in recorded COF with amplitudes  $4 \times 10^{-5}$  and  $3 \times 10^{-5}$  respectively, but there is no noise dependence during these peaks, neither any vibrations are observed in the accelerometer. Similar trend is observed in Figure 21 (c) for low humidity condition as well. Increase in humidity results in lowering the vibration in case of modal material 1. Similar decrease is observed in recorded noise by microphone.



(a)

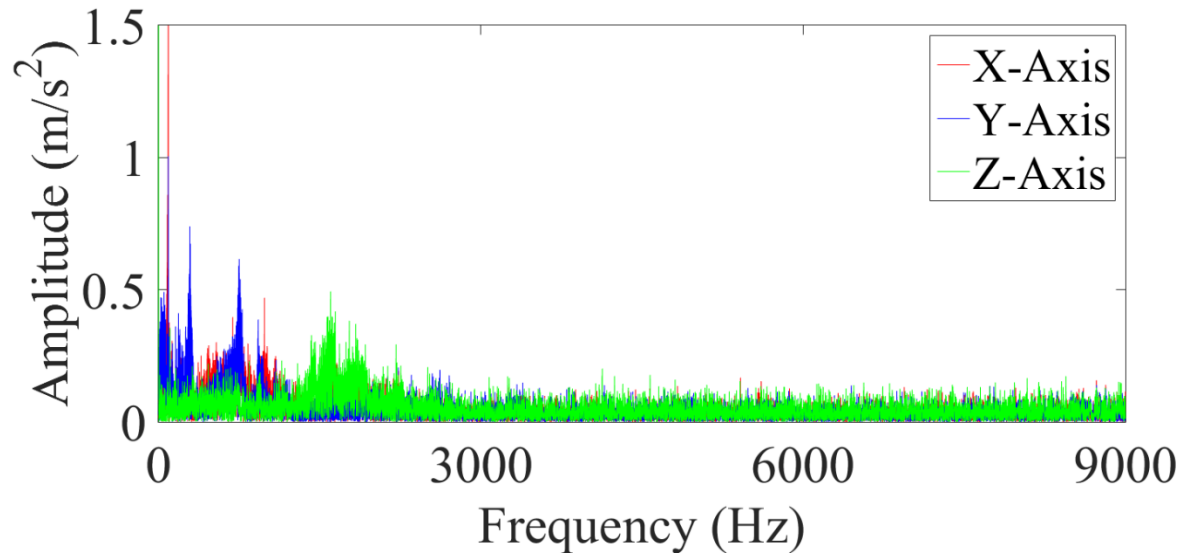


(b)

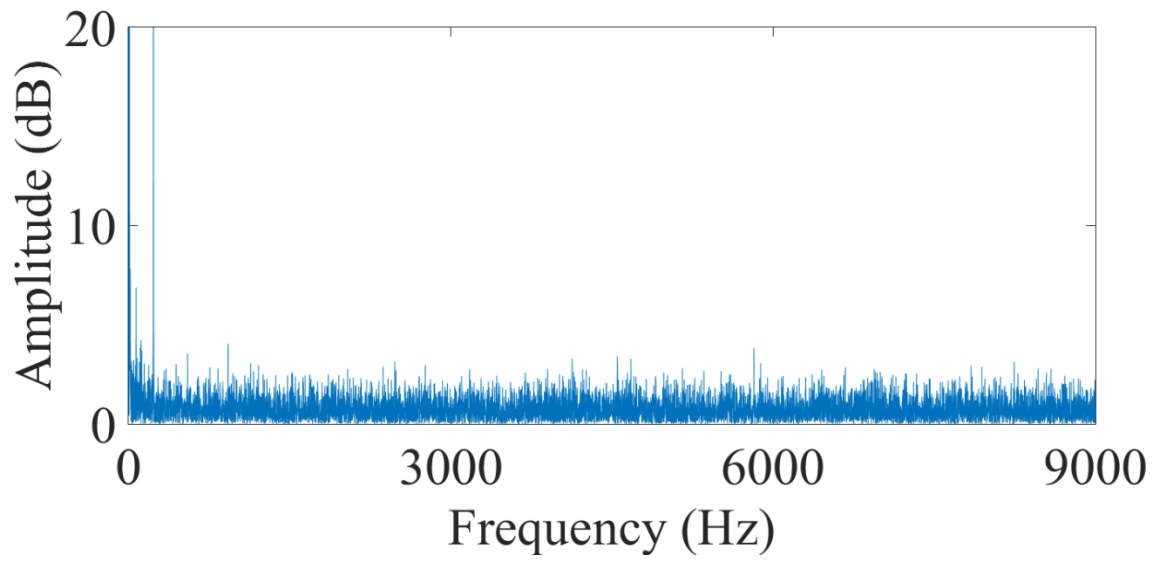


(c)

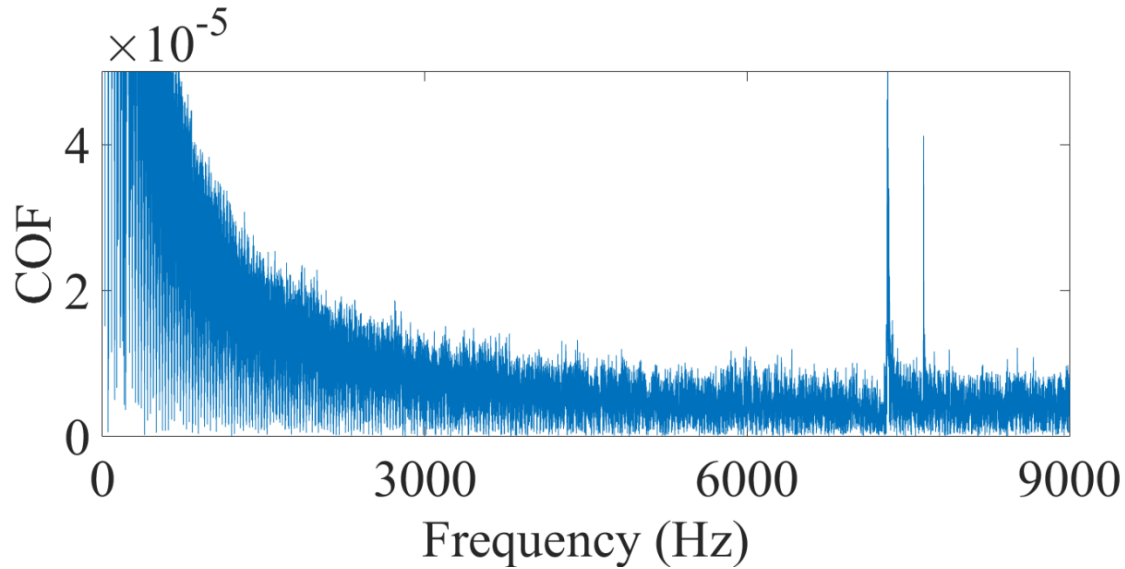
Figure 23 FFT analysis of accelerometer (a), microphone (b) and COF in UMT (c) for modal material 2 at 15%RH



(a)



(b)



(c)

Figure 24 FFT analysis of accelerometer (a), microphone (b) and COF in UMT (c) for modal material 2 at 65%RH

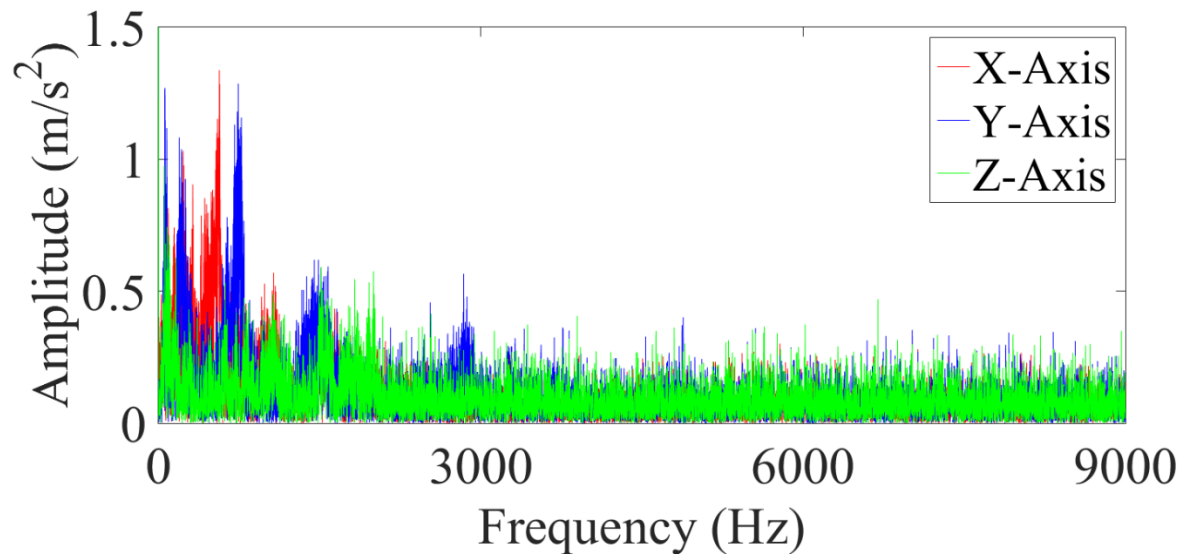
Figure 23 (a) represent the accelerometer vibrations, 23 (b) represent the noise recorded and 23 (c) represent the distribution of COF for modal material 2 at low humidity level. Significant vibrations are observed initially during the engagement with an amplitude range of (0-0.5)  $\text{m/s}^2$ . Microphone recorded data with amplitude near to 20dB in the initial stage, during the engagement of samples with the rotor. In between 6000Hz and 9000Hz frequency peaks are observed in recorded COF with amplitudes  $4 \times 10^{-5}$  more respectively, but there is no noise dependence during these peaks, neither any vibrations are observed in the accelerometer.

Figure 24 (a) represent the accelerometer vibrations, 24 (b) represent the noise recorded and 24 (c) represent the distribution of COF for modal material 2 at high humidity level. Vibrations are observed at 2000Hz frequency with an amplitude of 0.5  $\text{m/s}^2$ , but there is no noise recorded during these vibrations. Few peaks are observed at 3000Hz and 5000Hz frequency with an amplitude of 1  $\text{m/s}^2$  and 0.75  $\text{m/s}^2$  respectively. But, there is no noise recorded by the

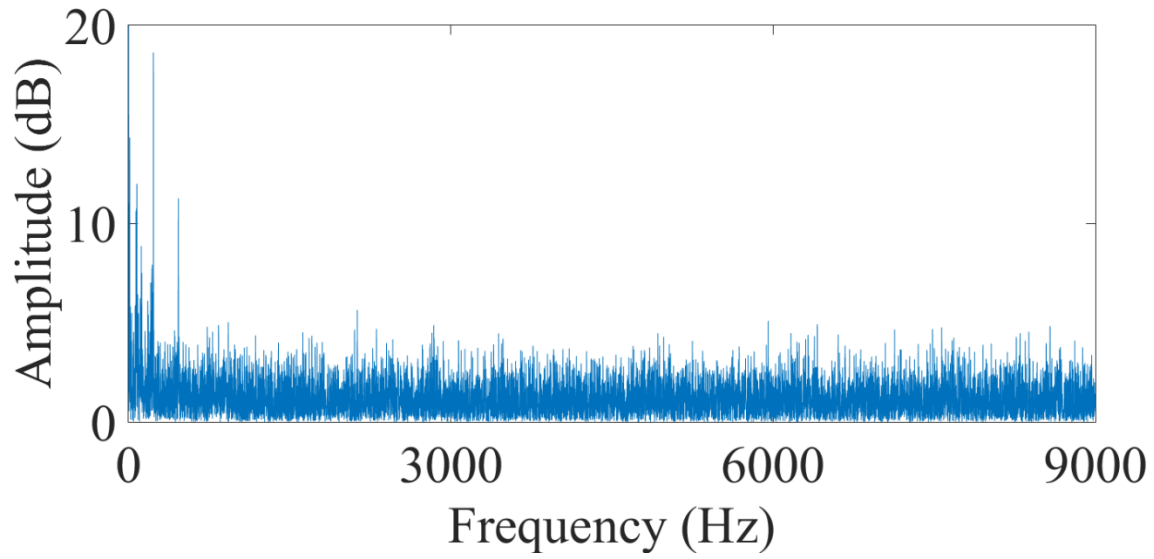
microphone at these peaks, microphone recorded data with amplitude near to 20dB in the initial stage, during the engagement of samples with the rotor. In between 6000Hz and 9000Hz frequency peaks are observed in recorded COF with amplitudes  $4 \times 10^{-5}$  and  $3 \times 10^{-5}$  respectively, but there is no noise dependence during these peaks, neither any vibrations are observed in the accelerometer, Similar trend is also observed in case of low humidity. The overall amplitude of vibration and noise response is decreased at higher humidity level. In case of real braking change in humidity effects the frictional performance of NAO brake pads, in which they perform considerably well at higher humidity levels.

Drag test:

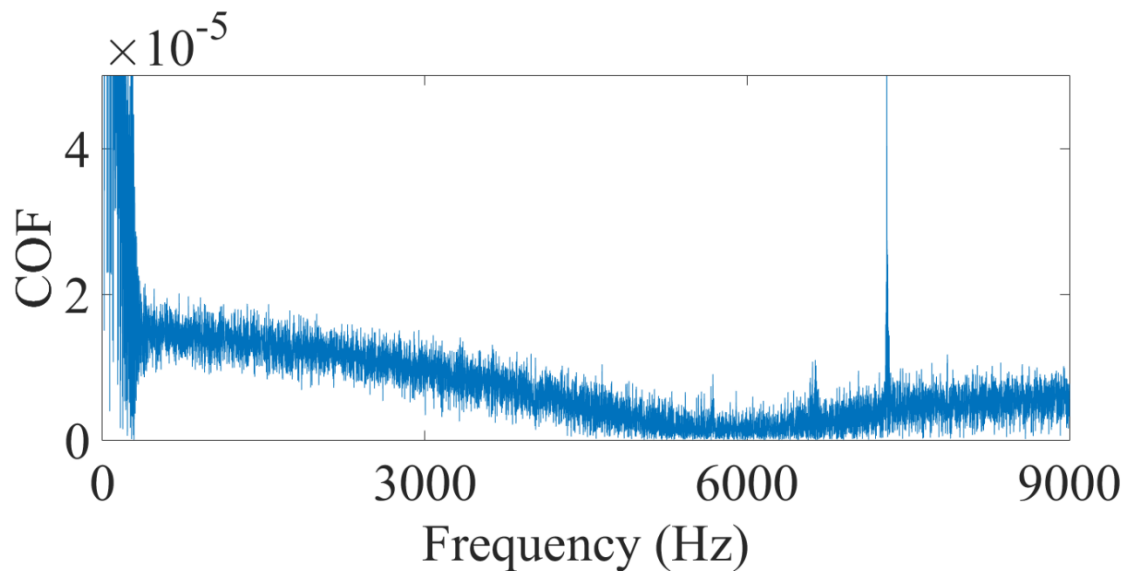
Accelerometer vibration data, microphone noise data and the COF data collected in case of Drag test for each model brake at different relative humidity levels are plotted in Figures 25, 26, 27 and 28 respectively.



(a)

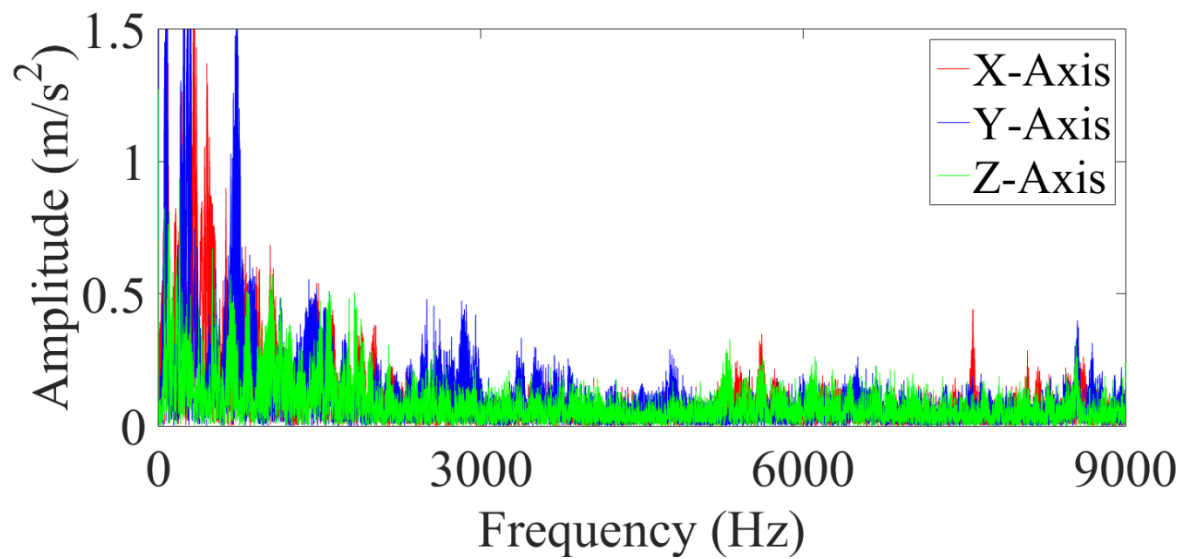


(b)

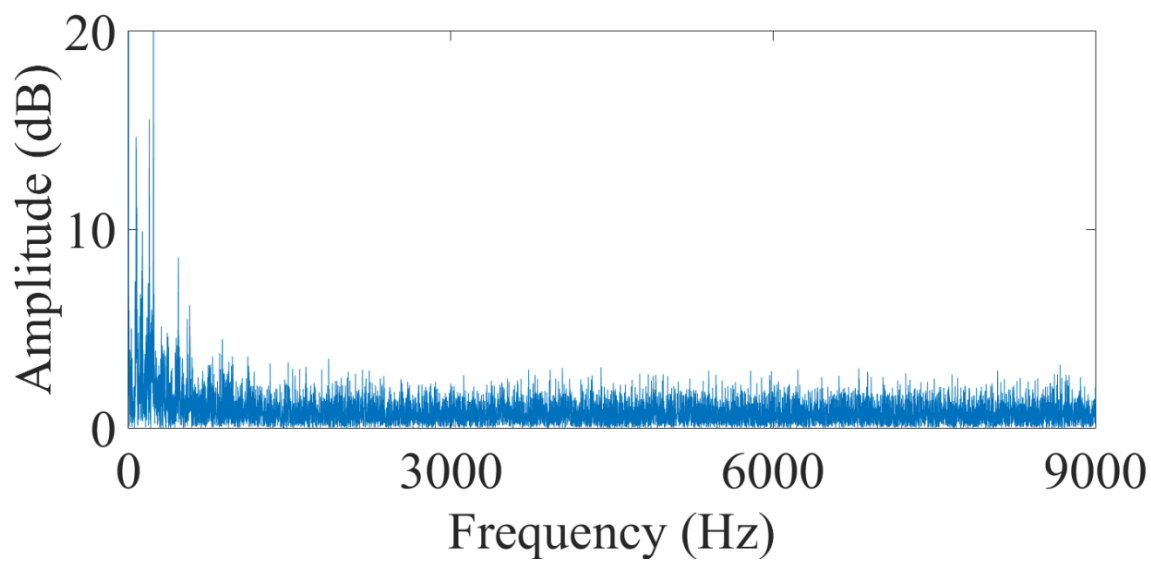


(c)

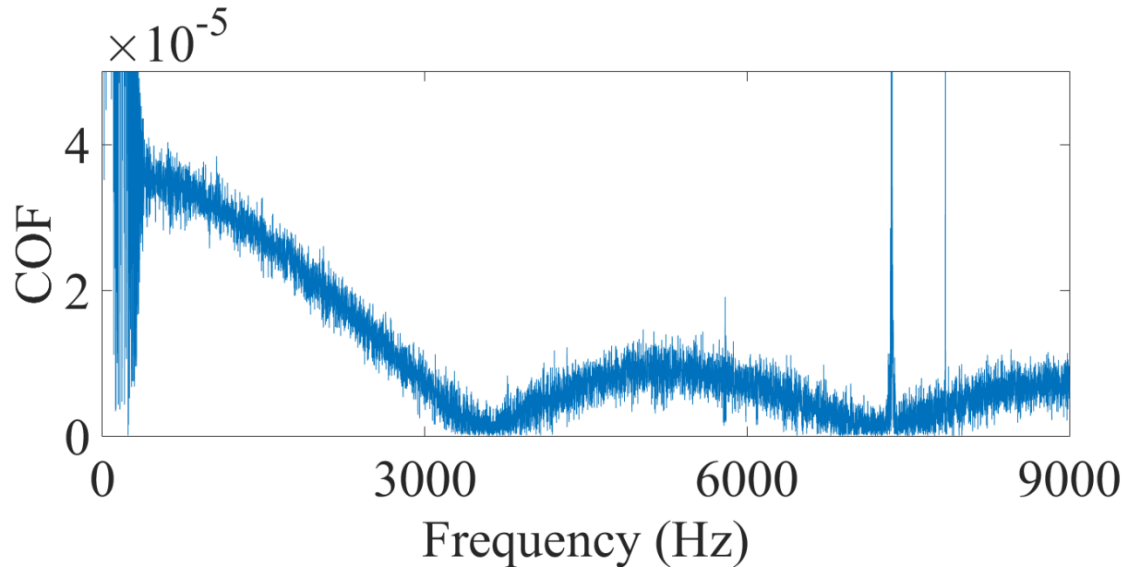
Figure 25 FFT analysis of accelerometer (a), microphone (b) and COF in UMT (c) for modal material 1 at 15%RH



(a)



(b)



(c)

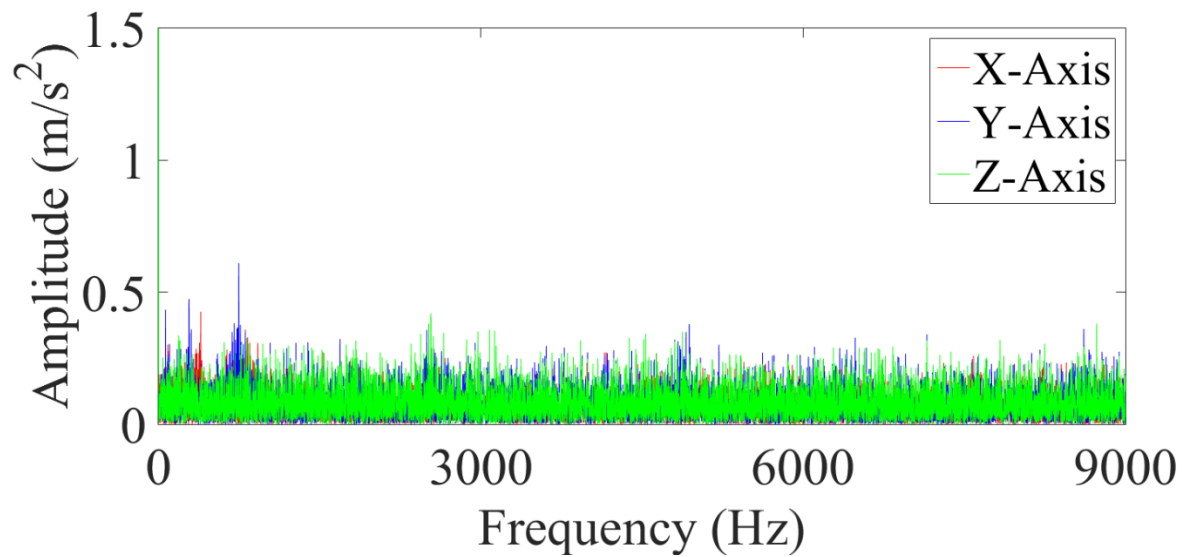
Figure 26 FFT analysis of accelerometer (a), microphone (b) and COF in UMT (c) for modal material 1 at 65%RH

Figure 25 (a) represent the accelerometer vibrations, 25 (b) represent the noise recorded and 25 (c) represent the distribution of COF for modal material 1 at low humidity level. Significant vibrations are observed in all the 3 axes, initially during the engagement with an amplitude range of  $(0.5-1) \text{ m/s}^2$ . Few peaks are observed at 3000Hz frequency with an amplitude of  $0.5 \text{ m/s}^2$ , but there is no noise recorded by the microphone at the respective peak, microphone recorded data with amplitude near to 20dB in the initial stage, during the engagement of samples with the rotor. In between 6000Hz and 9000Hz frequency COF vibrated with an amplitude of  $4 \times 10^{-5}$ , but there is no noise dependence during these peaks, neither any vibrations are observed in the accelerometer.

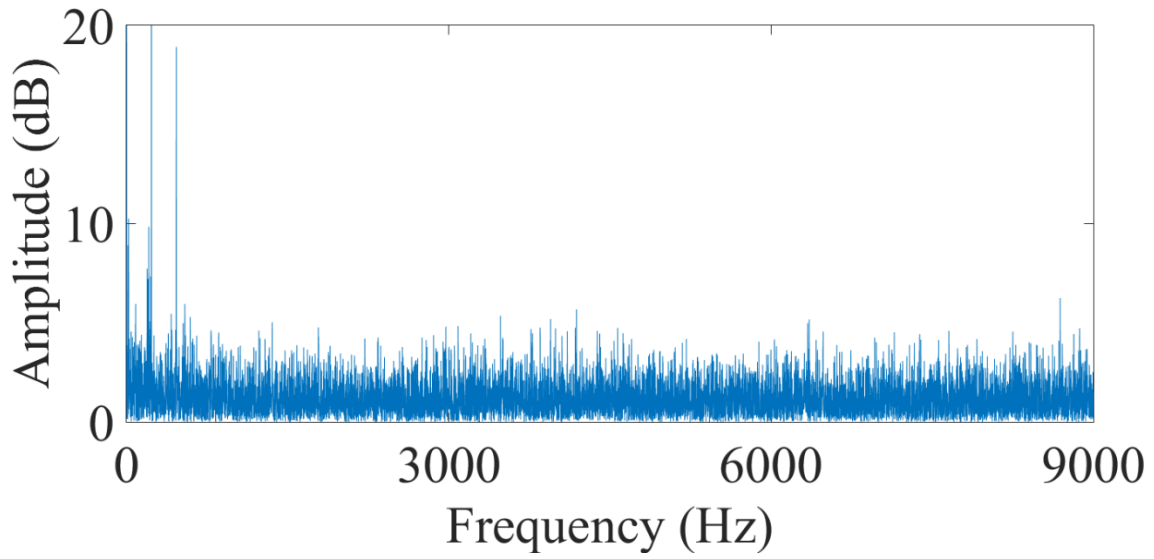
Figure 26 (a) represent the accelerometer vibrations, 26 (b) represent the noise recorded and 26 (c) represent the distribution of COF for modal material 1 at high humidity level. Significant vibrations are observed initially during the engagement with an amplitude range of value greater than  $1 \text{ m/s}^2$ . Few peaks are observed at 3000Hz, 8000Hz and 9000Hz frequency



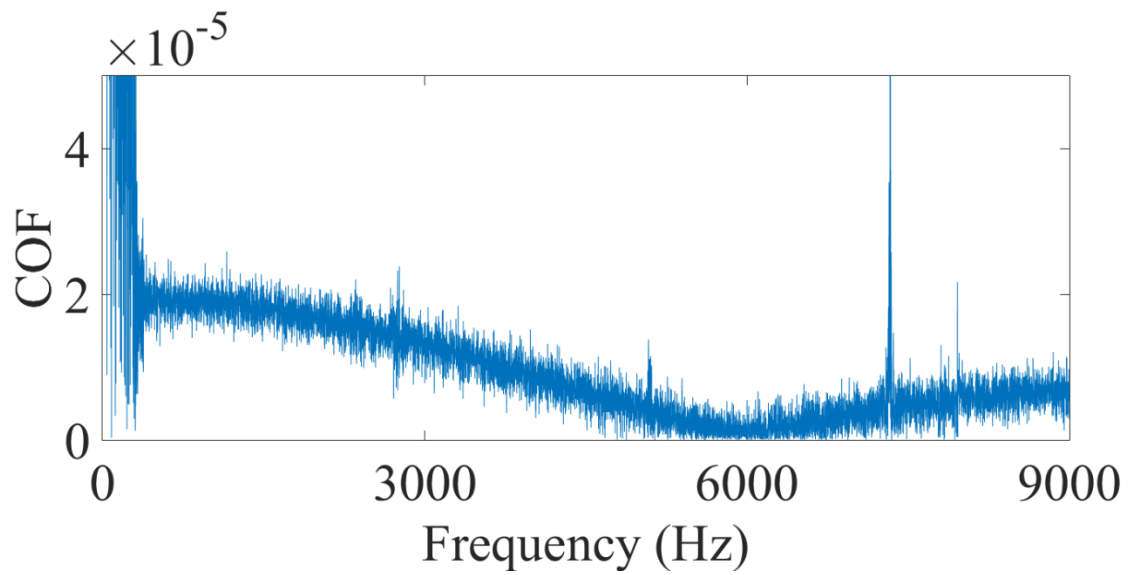
with an amplitude of  $0.75 \text{ m/s}^2$ . But, there is no noise recorded by the microphone at these peaks, microphone recorded data with amplitude near to 20dB in the initial stage, during the engagement of samples with the rotor. In between 6000Hz and 9000Hz frequency peaks are observed in recorded COF with amplitudes  $4 \times 10^{-5}$  and  $3 \times 10^{-5}$  respectively, but there is no noise dependence during these peaks, neither any vibrations are observed in the accelerometer. By comparing Figures 25 (c) and 26 (c) it is clearly observed that COF has different vibrations at different humidity levels, but neither of them show any dependency over noise. In case of drag test, increase in humidity has impact on vibrations in COF for LS brake pads.



(a)

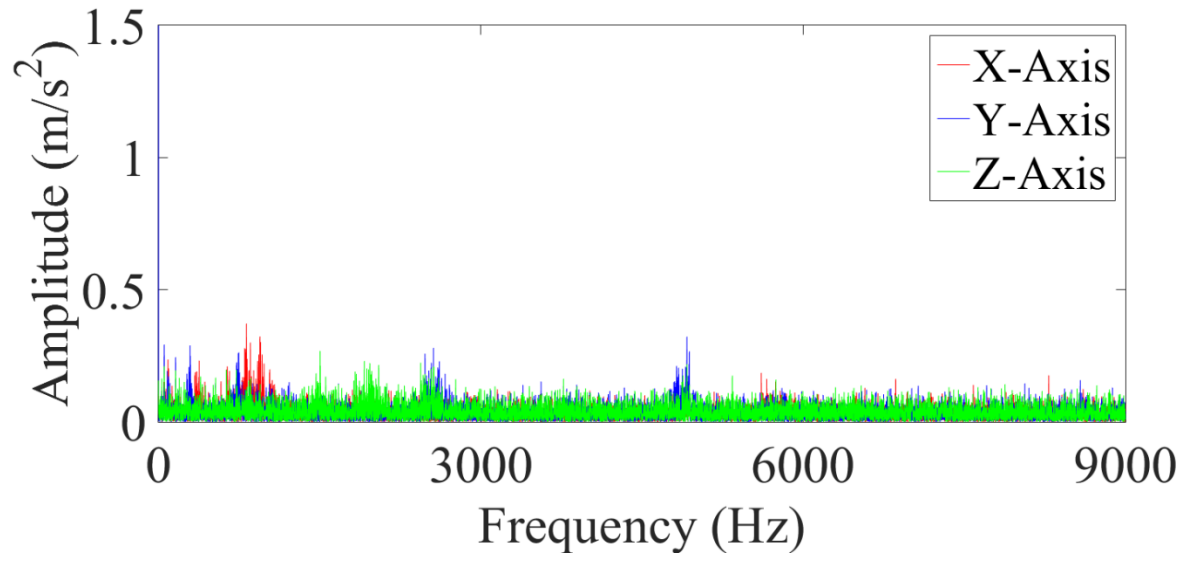


(b)

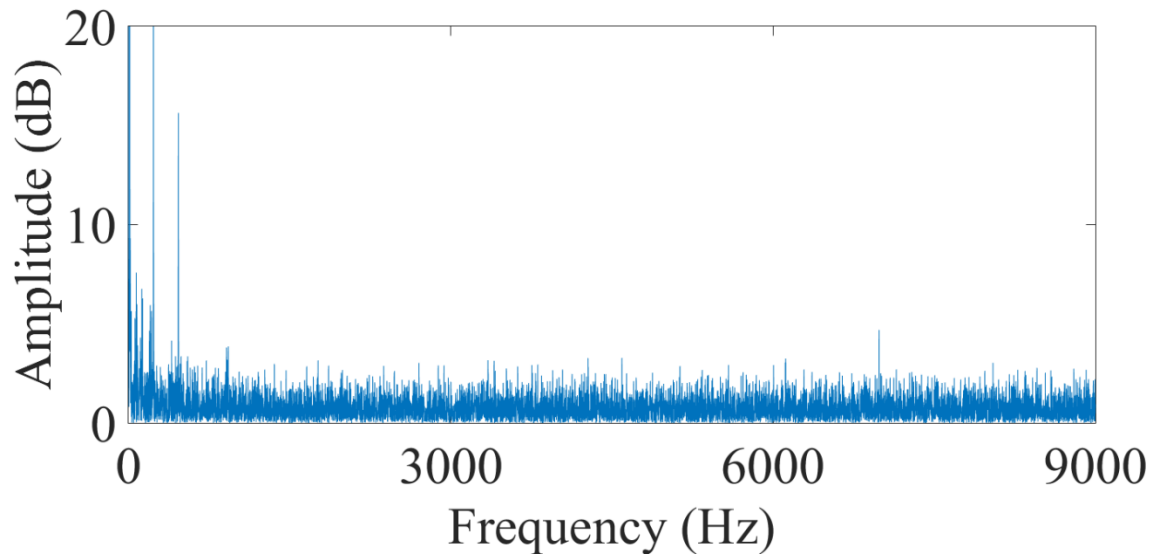


(c)

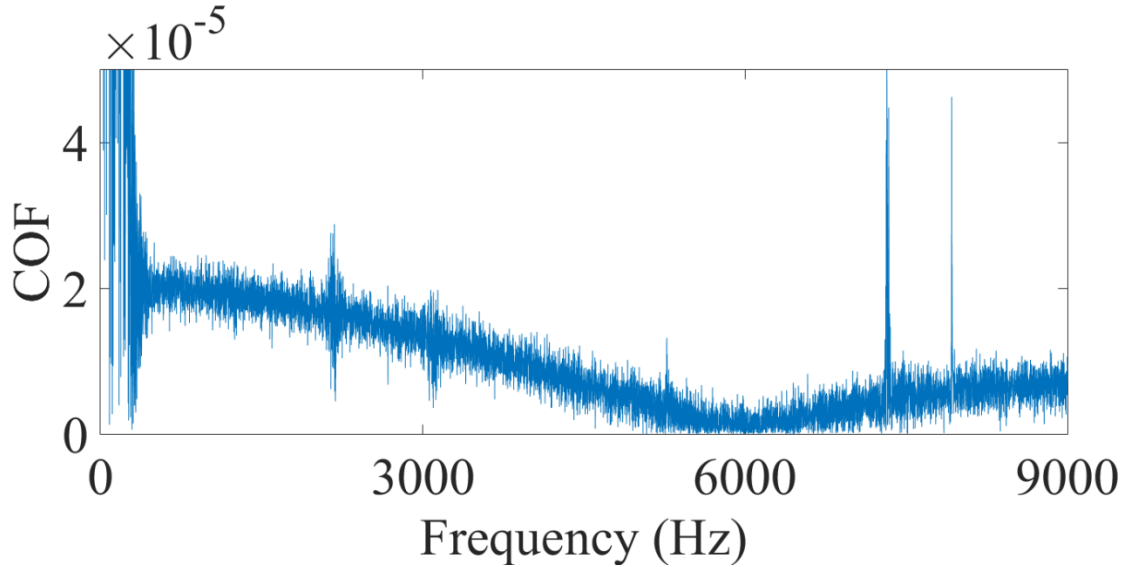
Figure 27 FFT analysis of accelerometer (a), microphone (b) and COF in UMT (c) for modal material 2 at 15%RH



(a)



(b)



(c)

Figure 28 FFT analysis of accelerometer (a), microphone (b) and COF in UMT (c) for modal material 2 at 65%RH

Figure 27 (a) represent the accelerometer vibrations, 27 (b) represent the noise recorded and 27 (c) represent the distribution of COF for modal material 2 at low humidity level. Few vibrations are observed in all the Y-axes, initially during the engagement with an amplitude range of  $0.5 \text{ m/s}^2$ . Few peaks are observed at 3000Hz frequency with an amplitude of  $0.5 \text{ m/s}^2$ , but there is no noise recorded by the microphone at the respective peak, microphone recorded data with amplitude near to 20dB in the initial stage, during the engagement of samples with the rotor. At 300Hz, 6000Hz and 9000Hz frequency COF vibrated with an amplitude of  $1 \times 10^{-5}$  and  $4 \times 10^{-5}$  respectively, but there is no noise dependence during these peaks, neither any vibrations are observed in the accelerometer.

Figure 28 (a) represent the accelerometer vibrations, 28 (b) represent the noise recorded and 28 (c) represent the distribution of COF for modal material 2 at high humidity level. No Significant vibrations are observed initially during the engagement when compared with. Few

peaks are observed at 3000Hz, 8000Hz and 9000Hz frequency with an amplitude of  $0.75 \text{ m/s}^2$ .

But, there is no noise recorded by the microphone at these peaks, microphone recorded data with amplitude near to 20dB in the initial stage, during the engagement of samples with the rotor.

Peaks are observed at 2000Hz, 3000Hz and in between 6000Hz and 9000Hz in recorded COF but there is no noise dependence during these peaks, neither any vibrations are observed in the accelerometer. By comparing Figures 25 (c) and 26 (c) it is clearly observed that COF has different vibrations at different humidity levels, but neither of them show any dependency over noise. As humidity increases, the COF vibrations also increases, similar trend is observed in case of modal material 1 for Drag test. By comparing figures 27 (a) and 28 (a), vibrations are reduced by increase in humidity and performs well at higher humidity conditions which is also observed in Real Braking condition.

## CHAPTER 6

### CONCLUSION

1. Increase of relative humidity increased the level of detected coefficient of friction.
2. LM brake pad has larger differences in COF with varying humidity conditions when compared with NAO brake pad.
3. During braking process, the real contact takes place at elevated areas on the surfaces. Those plateaus, groves and sliding direction are observed in SEM images.
4. Real braking simulation and drag tests generate completely different results.
5. Due to the presence of nano-additives, friction induced vibrations at higher humidity conditions are reduced.
6. It is observed that if there are oscillations in friction levels and if we observe vibration in system. It does not necessarily mean that there is always a noise.

## REFERENCES

- [1] P. J. Blau, "Compositions, functions, and testing of friction brake materials and their additives," *Oak Ridge National Lab*, 2001.
- [2] I. Barys Shyrokau, "Vehicle dynamics with brake hysteresis," *Proceedings of the Institution of Mechanical Engineers, Part D: Journal of Automobile Engineering* , vol. 227, no. 2, pp. 139-150, 2012.
- [3] A. Bonfanti, *Low-impact friction materials for brake pads*, University of Trento, 2016.
- [4] B. J. B. Karlheinz Bill, *Brake Technology Handbook*, SAE International, 2008.
- [5] K.Deepika, "Fabrication and performance evaluation of a composite material for wear resistance application," *IJESIT*, vol. 2, no. 6, pp. 66-71, 2013.
- [6] P. Filip, *Frcition science and Applications*, Carbondale, 2017.
- [7] R. R. Boyna, P. Filip, "IMPACT OF FRICTION TEST SCALE ON BRAKE FRICTION PERFORMANCE," *Opensiuc* , 2016.
- [8] P. F. T. Policandriotes, "Effects of selected nanoadditives on the friction and wear performance of carbon–carbon aircraft brake composites," *Wear*, vol. 271, no. 9-10, pp. 2280-2289, 2011.
- [9] S.S. W. Gajek, "Some tribological characteristics of disc brake pads," *Automotive Archive*, vol. 3, pp. 33-46, 2012.
- [10] N. Axen, "Friction and Wear Measurment Techniques," CRC Press, 2001.
- [11] F. B. S. J. Mikael Eriksson, "On the nature of tribological contact in automotive brakes," *Wear*, vol. 252, no. 1-2, pp. 26-36, 2002.
- [12] F. Talati and S. Jalalifar, "Analysis of heat conduction in a disk brake system," *Heat & Mass Transfer*, no. 45, pp. 1047-1059, 2009.
- [13] M. Eriksson, F. Bergman and S. Jacobson, " On the nature of tribological contact in automotive brakes," *Wear*, no. 252, pp. 26-36, 2002.
- [14] P. F. Saereh Mirzababaei, "Impact of humidity on wear of automotive friction materials," *Wear*, vol. 376–377, no. ISSN 0043-1648, pp. 717-726, 2017.
- [15] H. J. e. al., "Frictional instability induced by iron and iron oxides on friction material surface," *Wear*, Vols. 400-401, pp. 93-99, 2018.
- [16] D. Thuresson, "Thermomechanical analysis of friction brakes," *SAE Technical Paper*, p. 13, 2000.

- [17] G. W. S. D Chan, "Review of automotive brake friction materials.," *SAGE journals*, vol. 218, no. 9, pp. 953-966, 2004.
- [18] K. C. Soom AA, "Interactions Between Dynamic Normal and Frictional Forces During Unlubricated Sliding," *ASME. J. of Lubrication Tech*, vol. 105, no. 2, pp. 221-229, 1983.
- [19] R. R. Boyna, Peter Filip, *Impact of Friction test scale on brake friction performance*, Carbondale: opensiuuc, 2016.
- [20] S. M. A. Committee, *Metrication and SAE*, SAE Technical Paper Series, 1971.
- [21] H. Athari, Peter Filip, "FRICTION MATERIAL DOWNSCALING AND ITS EFFECT ON BRAKE SYSTEM PERFORMANCE," *Opensiuuc*, 2017.
- [22] A. M. M. Alireza B. Dariane, "Comparative Analysis of Evolving Artificial Neural Network and Reinforcement Learning in Stochastic Optimization of Multi-reservoir Systems," *Hydrological Sciences Journal*, vol. 61:6, no. 10.1080/02626667.2014.986485, pp. 1141-1156, 2016.
- [23] G. A, *Scaling laws*, Kanpur: IIT, 2011.
- [24] P. Filip, "The Frictional Performance of Carbon-Carbon Composite Materials in the Presence of Hydraulic Fluid, Runway Deicer Agent, Aircraft Deicer Agent and Sea-Salt Water," in *Mechanical Properties and Performance of Engineering Ceramics II: Ceramic Engineering and Science Proceedings*, Ceramic Engineering and Science Proceedings, 2008.
- [25] M. Djafri, "Effects of humidity and corrosion on the tribological behaviour of the brake disc materials,," *Wear*, vol. 321, pp. 8-15, 2014.
- [26] W. Z. R. D. Filip. P, "On friction layer formation in polymer matrix composite materials for brake applications," *Wear*, pp. 189-198, 2002.
- [27] D. Dowson, *History of Tribology*, 1998.
- [28] F. P. T. D. Bowden, *The Friction and Lubrication of Solids*, Oxford University, 1986.
- [29] S. Jacobson, *Tribologi. Karlebo-Serien, Liber Utbildning* (Text book in Swedish), 1996.
- [30] M. J. S. Eriksson, "Tribological surfaces of organic brake pads," *Tribal. Intern.*, vol. 33, pp. 817-827, 2000.
- [31] J. S. Eriksson, "Wear and contact conditions of brake pads -dynamical in-situ studies of pad on glass.," *Wear*, pp. 272-278, 2001.



- [32] L. Leine, "Stick-Slip Vibrations Induced by Alternate Friction Models," *Nonlinear Dynamics*, vol. 16, pp. 41-54, 1998.
- [33] S. M. Bettella, "Investigation of automotive creep groan noise with a distributed-source excitation technique," *Journal of sound and vibration*, vol. 255, pp. 531-547, 2002.
- [34] J. S. Yoon, "Effect of surface contact conditions on the stick–slip behavior of brake friction material," *Wear*, vol. 294, pp. 305-312, 2012.
- [35] F. H. Jang, "Compositional effects of the brake friction material on creep groan phenomena," *Wear*, vol. 251, no. 1, pp. 1477-1483, 2001.
- [36] W. K. Lee, "The influence of humidity on the sliding friction of brake friction material," *Wear*, vol. 302, no. 1, pp. 1397-1403, 2013.
- [37] J. J. Bikerman, "Adhesion in friction," *Wear*, vol. 39, no. 1, pp. 1-13, 1976.
- [38] Y. M. Irina Goryacheva, "A model of the adhesive component of the sliding friction force," *Wear*, vol. 270, no. 9-10, pp. 628-633, 2011.
- [39] B. Bhushan, *Introduction to tribology*, John Wiley & Sons, 2013.
- [40] L. Johnson, "Surface energy and the contact of elastic solids," *Proceedings of the Royal Society of London. A. Mathematical and Physical Sciences*, vol. 324, no. 1558, pp. 301-313, 1971.
- [41] D. Tabor, "Surface forces and surface interactions," *Journal of Colloid and Interface Science*, pp. 2-13, 1977.
- [42] G. C. J.-Y. C. Liangbiao Chen, "An Insight to High Humidity-Caused Friction Modulation of Brake by Numerical Modeling of Dynamic Meniscus under shearing," *Lubricants*, no. 3, pp. 437-446, 2015.
- [43] M. Kobayashi and N. Odani, "Study on Stabilization Friction Coefficient of Disk Brake Pads in Cold," *SAE Tech. Paper*, 1997.
- [44] M. Eriksson, A. Lundqvist and S. Jacobson, "A study of the influence of humidity on the friction and squeal generation of automotive brake pads," *J. Automob. Eng.*, no. 215, pp. 329-342, 2001.
- [45] J. F. K. Cho, "The size effect of zircon particles on the friction characteristics of brake lining materials," *Wear*, vol. 264, no. 3, pp. 291-297, 2008.
- [46] H. Cho, "Effects of ingredients on tribological characteristics of a brake lining: an experimental case study," *Wear*, vol. 258, pp. 1682-1687, 2005.

- [47] W. Osterle, "On the role of copper in brake friction material," *Tribology International*, vol. 43, pp. 2317-2326, 2010.
- [48] J. Bijwe, "Composites as friction materials: Recent developments in nonasbestos fiber reinforced friction materials—a review," *Polymer composites*, vol. 18, no. 3, pp. 378-396, 1997.
- [49] K.-T. Cheng, Peter Filip, *EFFECT OF NANOADDITIVES AND HUMIDITY ON FRICTION PERFORMANCE OF AUTOMOTIVE BRAKE MATERIALS*, Carbondale: Opensiuc, 2017.
- [50] J. Bijwe, "Nanoabrasives in friction materials-influence on tribological properties," *Wear*, vol. 296, no. 1, pp. 693-701, 2012.
- [51] X. Pei, "The influence of nanoparticle fillers on the friction and wear behavior of polymer matrices," *Tribology and Interface Engineering Series*, vol. 55, pp. 62-81, 2008.
- [52] E. J. Lee, "Morphology and toughness of abrasive particles and their effects on the friction and wear of friction materials: a case study with zircon and quartz," *Tribology Letters*, no. 37, pp. 637-344, 2007.
- [53] R. K. Jayashree Bijwe, "Nano-abrasives in friction materials-influence on tribological properties," *Wear*, pp. 693-701, 2012.
- [54] W. Li, "Friction and wear properties of ZrO<sub>2</sub>/SiO<sub>2</sub> composite nanoparticles," *Journal of Nanoparticle Research*, vol. 13, no. 5, pp. 2129-2137, 2011.
- [55] W. Ö. a. A. I. Dmitriev, "The Role of Solid Lubricants for Brake Friction Materials," *Lubricants*, vol. 4, p. 5, 2016.
- [56] R. R. Boyana, "IMPACT OF FRICTION TEST SCALE ON BRAKE FRICTION PERFORMANCE," Opensiuc, Carbondale, 2016.
- [57] P. Samyn, "Large-scale tests on friction and wear of engineering polymers for material selection in highly loaded sliding systems," *Materials and Design*, vol. 27, pp. 535-555, 2006.
- [58] A. G. Oliviero, "A laboratory brake for the study of automotive brake noise," *IMAC-XX: Conference & Exposition on Structural Dynamics*, pp. 548-551, 2002.
- [59] A. Abdul wahab, *Reduced scale thermal characterization of automotive disc brake*, Applied Thermal Engineering, 2014.
- [60] W. Fecher, "Caliper-independent investigation of brake pads," *EuroBrake*, 2014.

- [61] Z. Jiang, "Microforming Technology Theory, simulation and practice.," *Academic Press*, 2017.
- [62] Enker, *Introduction to Scaling laws*, JSD, 2007.
- [63] B. N. S. Division, "Efficiently Measuring Brake Materials," 2018. [Online]. Available: [www.bruker.com/BrakeMaterialTest](http://www.bruker.com/BrakeMaterialTest).
- [64] Z. a. D. P.Filip, "On friction layer formation in polymer matrix composite materials for brake applications," *Wear*, vol. 252, no. 3, pp. 188-198, 2002.
- [65] M.Eriksson, "Friction and contact phenomena of disc brakes related to squeal," *Citeseer*, 2002.
- [66] P. Blau, *Compositions, functions, and testing of friction brake materials and their additives*, TN (US): Oak Ridge National Lab, 2001.
- [67] G. S. D. Chan, "Review of automotive brake friction materials," *Journal of Automobile Engineering*, vol. 218, no. 9, pp. 953-966, 2004.
- [68] M. H. Cho, "Effects of ingredients on tribological characteristics of a brake lining: an experimental case study," *Wear*, vol. 258, no. 11, pp. 1682-1687, 2005.
- [69] K. T. STADLER Z., "Friction and wear of sintered metallic brake linings on a C/C-SiC composite brake disc.," *Wear*, no. 265, 2008.
- [70] C. H. J. SEONG J. K., "Complementary effects of solid lubricants in the automotive brake lining.," *Tribology international*, no. 40, 2007.
- [71] J. Balotin, P. Neis and N. Ferreira, "Analysis of the influence of temperature on the friction coefficient of friction materials.," in *ABCM Symposium Series in Mechatronics*, Rio de Janeiro, 2010.
- [72] S. J. Faramarz Talati, "Analysis of heat conduction in a disk brake system," *Heat and Mass Transfer*, vol. 45, p. 1047, 2009.
- [73] A. V. I. Barys Shyrokau, "Vehicle dynamics with brake hysteresis," *SAGE journals*, vol. 227, no. 2, pp. 139-150, 2012.
- [74] D. Hess and A. Soom, "Friction at a lubricated line contact operating at oscillating sliding velocities," *Tribology*, vol. 112, pp. 147-152, 1990.
- [75] R. S.N. Nagesh, "Characterization of Brake Pads by Variation in Composition of Friction Materials," *Procedia Materials Science*, vol. 5, pp. 295-302, 2014.
- [76] H. B.E, "Oxidation of metals and alloys," *Butterworths Scientific Publications*, 1953.

- [77] J. Gerlici, "Noise and temperature reduction in the contact of tribological elements during braking," in *MATEC Web of Conferences 157*, 2018.
- [78] A. Y. Wang, "Effect of surface roughness on friction-induced noise: Exploring the generation of squeal at sliding friction interface," *Wear*, Vols. 402-403, pp. 80-90, 2018.
- [79] H. Athari, *FRICITION MATERIAL DOWNSCALING AND ITS EFFECT ON BRAKE SYSTEM PERFORMANCE*, Opensiuc, 2017.
- [80] A. B. Dariane, "Comparative Analysis of Evolving Artificial Neural Network and Reinforcement learning in Stochastic Optimization of Multi-reservoir Systems," *Hydrological Sciences Journal*, vol. 61:6, pp. 11141-1156, 2016.
- [81] H. Athari, Peter Filip, "Friction Material Down Scaling and Its Effect on Brake Friction Performance," in *SAE brake colloquium*, Orlando, 2017.
- [82] M. Ziomek-Moroz, G. Holcomb, B. J. Covino, S. Bullard and P. & A. D. Jablonski, "Corrosion Performance of Ferritic Steel for SOFC Interconnect Applications," *Office of Scientific & Technical Information Technical Reports*, 2006.
- [83] K. P. F. Katarzyna Peszynska-Bialczyk, "Thermal analysis of bulk carbon-carbon composite and friction products derived from it during simulated aircraft braking.," *Carbon*, vol. 45, no. 3, pp. 524-530, 2007.
- [84] P. Hee, "Performance of ceramic enhanced phenolic matrix brake lining materials for automotive brake lining," *Wear*, vol. 259, pp. 1161-1096, 2005.
- [85] R. K. Talib Ria Jaafar, "Selection of Best Formulation for SemiMetallic Brake Friction Materials Development," *Powder Metallurgy*, 2012.
- [86] M. M. et, "Effect of Compressibility of Brake Friction Materials on vibration occurrence," *International Journal of Transport andd vehicle Engineering*, vol. 11, pp. 1776-1779, 2017.
- [87] K. Lee, P. Blau and J. Truhan, "Effects of moisture adsorption on laboratory wear measurements of brake friction materials," *Wear*, no. 262, pp. 925-930, 2007.

VITA  
Graduate School  
Southern Illinois University

Sai Krishna Kancharla

[kancharla369@gmail.com](mailto:kancharla369@gmail.com)

Jawaharlal Nehru Technological University,  
Bachelor of Technology in Mechanical Engineering,  
May 2016.

Thesis Title:

Effect of Humidity and testing strategy on Friction Performance of model brake pads  
containing Nano-additives

Major Professor: Dr. Peter Filip.